

# **PUBLICATIONS OF THE INSTITUTE OF GEOPHYSICS POLISH ACADEMY OF SCIENCES**

**Geophysical Data Bases, Processing and Instrumentation**

**439 (E-12)**

**BOOK OF EXTENDED ABSTRACTS**

**Webinar**

**on Methods for Ecohydraulics: Remote Sensing,  
17-20 May 2022**



**Warsaw 2022 (Issue 1)**

**INSTITUTE OF GEOPHYSICS  
POLISH ACADEMY OF SCIENCES**

**PUBLICATIONS  
OF THE INSTITUTE OF GEOPHYSICS  
POLISH ACADEMY OF SCIENCES**

**Geophysical Data Bases, Processing and Instrumentation**

**439 (E-12)**

**BOOK OF EXTENDED ABSTRACTS**

**Webinar**

**on Methods for Ecohydraulics: Remote Sensing,**

**17-20 May 2022**

**Warsaw 2022**

**Honorary Editor**  
Roman TEISSEYRE

**Editor-in-Chief**  
Marek KUBICKI

**Advisory Editorial Board**

Janusz BORKOWSKI (Institute of Geophysics, PAS)  
Tomasz ERNST (Institute of Geophysics, PAS)  
Maria JELEŃSKA (Institute of Geophysics, PAS)  
Andrzej KIJKO (University of Pretoria, Pretoria, South Africa)  
Natalia KLEIMENOVA (Institute of Physics of the Earth, Russian Academy of Sciences, Moscow, Russia)  
Zbigniew KŁOS (Space Research Center, Polish Academy of Sciences, Warsaw, Poland)  
Jan KOZAK (Geophysical Institute, Prague, Czech Republic)  
Antonio MELONI (Istituto Nazionale di Geofisica, Rome, Italy)  
Hiroyuki NAGAHAMA (Tohoku University, Sendai, Japan)  
Kaja PIETSCH (AGH University of Science and Technology, Cracow, Poland)  
Paweł M. ROWIŃSKI (Institute of Geophysics, PAS)  
Steve WALLIS (Heriot Watt University, Edinburgh, United Kingdom)  
Wacław M. ZUBEREK (University of Silesia, Sosnowiec, Poland)

**Associate Editors**

Łukasz RUDZIŃSKI (Institute of Geophysics, PAS) – **Solid Earth Sciences**  
Jan WISZNIEWSKI (Institute of Geophysics, PAS) – **Seismology**  
Jan REDA (Institute of Geophysics, PAS) – **Geomagnetism**  
Krzysztof MARKOWICZ (Institute of Geophysics, Warsaw University) – **Atmospheric Sciences**  
Mark GOŁKOWSKI (University of Colorado Denver) – **Ionosphere and Magnetosphere**  
Andrzej KUŁAK (AGH University of Science and Technology) – **Atmospheric Electricity**  
Marzena OSUCH (Institute of Geophysics, PAS) – **Hydrology**  
Adam NAWROT (Institute of Geophysics, PAS) – **Polar Sciences**

**Managing Editor**  
Anna DZIEMBOWSKA

**Technical Editor**  
Marzena CZARNECKA

Published by the Institute of Geophysics, Polish Academy of Sciences

ISBN 978-83-66254-10-7 eISSN-2299-8020  
DOI: 10.25171/InstGeoph\_PAS\_Publs-2022-001

Photo on the front cover by Roser Casas-Mulet

Editorial Office  
Instytut Geofizyki Polskiej Akademii Nauk  
ul. Księcia Janusza 64, 01-452 Warszawa

## C O N T E N T S

Preface .....	3
K. Alfredsen – Experiences with LiDAR and aerial imagery for the assessment of winter habitat, hydraulic modelling and riverscape classification .....	5
A.M. O’Sullivan – A picture speaks a thousand words: remote sensing in ecohydraulics .....	9
S. Dugdale – Remote sensing of river temperature in a changing climate: from knowledge to applied river management .....	11
N.J. Porter – Can you hear me now? An overview of telemetry technologies and their applications .....	13
L. Schmalfluss, M. Schletterer, and C. Hauer – Hydraulic modeling of a glacial lake outburst flood (GLOF) scenario at the River Biya .....	15
D. Farò, K. Baumgartner, R. Klar, A. Andreoli, F. Comiti, M. Aufleger, and G. Zolezzi – Integrating remote sensing and 2D hydraulic modelling for meso-habitat modelling in the Aurino, a gravel-bed Alpine river .....	19
M. Gargiulo, C. Cavallo, M.N. Papa, G. Ruello, and M. Nones – Deep learning approach for river hydro-morphodynamics monitoring using SAR data .....	23
M. Redana and L.T. Lancaster – Accurate estimation of water temperature from UAV-mounted thermal camera: the use of generalized additive models and dynamic programming algorithm to correct for vignetting effect and thermal shift .....	27
A.B. Alphonse and K. Kilingar Nadumane – Geographical Information System based morphometric analysis of Dibang River, Arunachal Pradesh, India .....	31
B. Baschek, E. Rommel, F. Kathöfer, L. Giese, K. Fricke, T. Mölter, F. Dzunic, M. Asgari, P. Nätke, P. Deffert, R. Gilles, J. Bongartz, A. Burkart, M. Heuner, I. Quick, and U. Schröder – Mapping riparian vegetation and hydromorphology with UAS and machine learning .....	35
C. Wu, M.J. Stewardson, J.A. Webb, and S. Norra – Modelling vegetation condition using a water balance model and long short-term memory networks on a floodplain receiving environmental water .....	39
L. Kirchgässner and G. Unfer – Evaluation of restoration projects with hyperspatial remote sensing of fish habitat using an Unmanned Aerial Vehicle (UAV) .....	43
Y. Zhou, Y. Zhang, Y. Han, and H. Liu – Experimental study on swimming behaviour of fish in an open channel based on video recognition .....	47
H. Liu, Y. Han, Y. Zhou, and Y. Zhang – Study on fish swimming behavior based on image velocimetry .....	53
J. Godfroy, J. Lejot, L. Demarchi, K. Michel, and H. Piegay – Processing of hyperspectral aerial images to characterise the bathymetry of rivers .....	57

## **Methods for Ecohydraulics: Remote Sensing**

### **PREFACE**

Habitat modeling has become a necessary tool in evaluating the status of water environments and to support the development of strategies and plans for improving their ecological status, guaranteeing ecological benefits and reducing anthropogenic effects. Despite the rapid growth of numerical models, in both hydraulic (hydraulic and morphological models) and biological (e.g., bio-energetic and individual based models) modeling, their application to fluvial systems remains hindered by a lack of supporting data at spatial scales larger than a single reach or at temporal scale beyond steady state or single event, as well as data necessary for model performance evaluation.

Recent advances – especially in remote sensing – may help to address this data need. These advances may include – but not limited to – technique using satellite and airborne devices (e.g., topo-bathymetric surveys, discharge, water surface elevation, water temperature and surface velocity, organisms' distribution including vegetation, fish and macro-invertebrate) and or telemetry.

The present work aims to summarize the outcomes of the webinar on Remote Sensing in Ecohydraulics, co-organized by the Institute of Geophysics of the Polish Academy of Sciences, the IAHR Committee on Ecohydraulics, the IAHR Poland Young Professional Network and ECoENet.

During the webinar, four keynote lectures and twelve technical notes, mainly coming from young researchers, provided the framework of the state-of-the-art of new tools, methods, equipment and methodologies for monitoring water habitats, and they aimed to share knowledge and address data survey needs.

In terms of the geographical distribution of the abstracts, more than 10 countries were represented, showing the worldwide importance of the topic, and the willingness for developing international and transdisciplinary connections.

We would like to acknowledge the contribution of the Scientific Committee and the Advisory Committee, which helped in assessing the abstracts, suggesting changes and future directions that, hopefully, can contribute to new outcomes and to filling gaps in using non-contact methods and techniques to address current issues in ecohydraulics.

*Local Organizing Committee*

Michael Nones  
Daniele Tonina  
Agata Keller  
Roser Casas-Mulet  
Baptiste Marteau  
Rafael O. Tinoco

# Experiences with LiDAR and Aerial Imagery for the Assessment of Winter Habitat, Hydraulic Modelling and Riverscape Classification

Knut ALFREDSEN

Norwegian University of Science and Technology,  
Department of Civil and Environmental Engineering, Trondheim, Norway

✉ Knut.Alfredsen@ntnu.no

## Abstract

The growing availability of remote sensed data provides new opportunities for analysis of conditions in lakes and rivers. Scanned terrain and bathymetry from LiDAR, various kind of satellite and aerial imagery and climatic data from satellite and combined products provide both a spatial and temporal resolution that is unavailable in traditional measurement approaches. Examples of use is drones and structure from motion to map ice formation and remnants in rivers. Effects of river ice is important for instream habitat in cold climate rivers and notoriously difficult to measure. Topographic and bathymetric LiDAR is used to build terrain models as a foundation for hydraulic modelling, providing highly detailed and accurate models. Finally, machine learning is used to classify historical aerial imagery providing a basis for the evaluation of the development of rivers.

**Keywords:** LiDAR, aerial imagery, hydraulic modelling, winter habitat, environmental assessment.

## 1. INTRODUCTION

Many analyses in eco-hydraulics require accurate spatial and temporal data. Recent developments in remote sensing techniques have opened new possibilities for a multitude of analysis, and data with better spatial and temporal resolution are becoming readily available. Data are both available from satellite and other larger aerial platforms, but the increasing availability of relatively low-cost drones with cameras and other instruments also opens possibilities for collecting remote sensed data on our own. This abstract briefly summarizes some applications.

## 2. EXAMPLES OF REMOTE SENSING APPLICATIONS

### 2.1 Using drones and structure from motion for winter habitat assessment

Instream habitat in winter in cold climate regions is strongly controlled by the formation of different forms of river ice, and the break-up of river ice can create sudden alterations to flow conditions and scouring of the riverbed from drifting ice. Mapping river ice can be a difficult undertaking since access to the ice in rivers can be difficult and at times even dangerous. For larger rivers, satellite imagery is commonly used to describe river ice on large scales, but for smaller rivers or cases where detail is needed the resolution of satellite images might not be adequate. Combining drone imagery and structure from motion allows for the creation of digital terrain models of various types of ice forming on the rivers (Alfredsen et al. 2018). This DEM could be used to evaluate ice forms and ice masses in rivers (Rødtang et al. 2021), provide input to hydraulic modelling and used to evaluate the ice impacts on flow and available habitats. The drone-based approach provides a fast and safe sampling method and through successive measurements the formation and decay of river ice can be quantified. Figure 1 shows an orthophotomosaic of anchor ice formation in the river Sokna in Norway. The damming effect of the ice significantly transform the depth and velocity distribution in the river section and alters the available habitat in a period with dropping or near constant discharge.

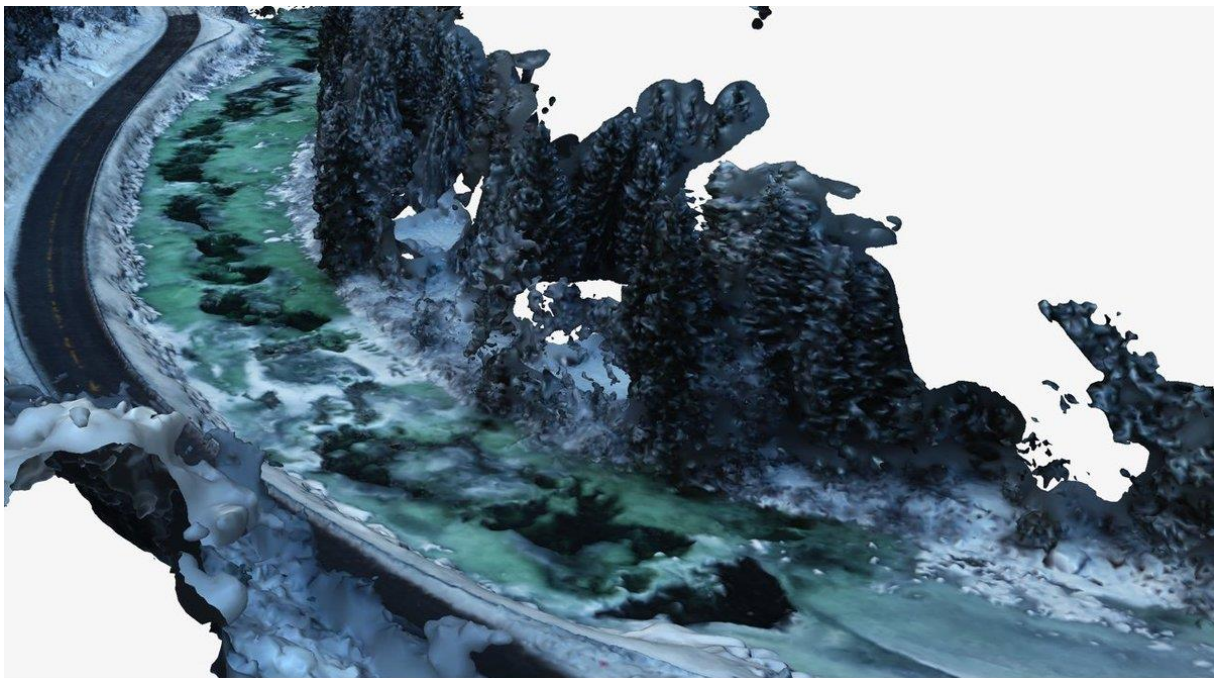


Fig. 1. Drone imagery of anchor ice damming a section of the river Sokna in Norway.

### 2.2 Using bathymetric LiDAR for hydraulic modelling

Hydraulic modelling has many applications in eco-hydraulics and have been used since the initial tools for the assessment of physical habitats were developed several decades ago. Providing data in adequate detail for the hydraulic simulation tools can be a challenge, and it can be time consuming and costly. The advent of bathymetric LiDAR provides a tool that can create highly detailed elevation models of rivers suitable for several different applications. Juarez et al. (2019) used a detailed LiDAR bathymetry and a hydraulic model of the Storåne river in Norway to predict ramping rates and dried out areas downstream of the Hol 1 power plant during peaking operation. The model was evaluated against measured water levels and water

covered areas from aerial imagery and provided an accurate description of the wetted areas for the range of the production discharges of the power plant. The results from the modelling study was used to propose an alternative operational regime that would reduce the stranding potential for fish in the dried out areas.

Historically, weirs have been used as a compensation measure in several regulated rivers in Norway to maintain water covered areas for several different reasons including ecology, visual aesthetics, recreational fishing and to keep ground water levels in adjacent farmlands. Recently the effects of weirs have been questioned, and possible negative effects on migration of fish and quality of habitat have been raised. Removal or adjustments of weirs have been done, and the precise terrain description available from LiDAR data can be utilised in assessing the effect of weir removal projects (Brekke 2020; Junker-Köhler and Sundt 2021). Through modelling the weir and different adjustment options the effect of the changes can be assessed both upstream and downstream the weir providing input for the planning process of the removal. The precise elevation models obtained through the bathymetric LiDAR is also promising related to sediments and the assessment of the geomorphology of rivers.

### 2.3 Historical development of rivers

Anthropogenic factors influence the development of rivers and is acknowledged as a major driver for impacts on biodiversity, and the UN has dedicated the coming decade to ecosystem restoration. Knowing the historical development of rivers is important for untangling the various forcing's driving change, but such data can be hard to find. Utilising the Norwegian repository of black and white aerial imagery ([www.norgebilder.no](http://www.norgebilder.no)) we used a convolutional neural network (CNN) to classify the riverscape over several decades in a number of rivers in Norway (Alfredsen et al. 2021). The training data set consisted of an initial set of images from two rivers that was manually annotated. The annotated images were used to create an initial trained model was then used to segment a third river, and the result from this segmentation process was then manually corrected and added to the training data to form an expanded dataset. The expanded dataset was then used to train and validate a second model. This model was then tested on data not used in the training process and the goodness of fit was evaluated using confusion matrices, an example from river Gaula in 1963 in Table 1.

Table 1  
Confusion matrix for Gaula in 1963

		Predicted [%]				
		Water	Gravel	Vegetation	Farmland	Human
True [%]	Water	91.31	0.38	1.38	2.39	0.28
	Gravel	7.84	76.73	6.72	10.07	6.05
	Vegetation	2.10	1.75	88.96	4.59	1.64
	Farmland	0.60	2.49	8.37	96.79	0.27
	Human	2.85	2.19	7.34	14.15	82.96

The trained CNN is used to generate segmented datasets for a number of rivers which are the fundament for the evaluation of the impact of human (e.g. hydropower, flood control, agriculture) and natural (e.g. floods) on the rivers. An example of river Nea from 1963 is shown in Fig. 2. We find that the CNN effectively replaces the tedious and time-consuming job of manually annotating the maps, leaving only minor manual corrections needed.

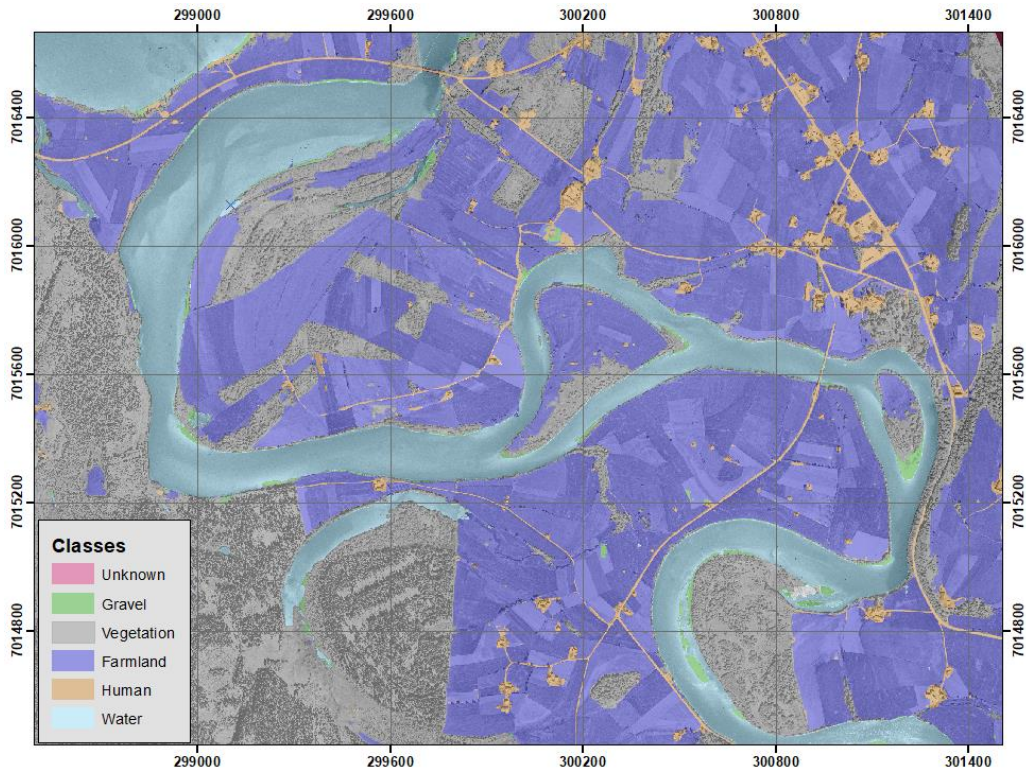


Fig. 2. Classified riverscape for river Nea overlaid aerial imagery from 1962.

**Acknowledgments.** I would like to thank Einar Rødtang, Ana Bustos, Ana Juárez, Etienne Limpens, Mahmoud Awadallah, Håkon Sundt, Jo Halvard Halleraker, Saeid Shamsaliei, Arild Dalsgård and Odd Erik Gundersen. I also wish to thank Morten Stickler for funding and the initiation of many interesting projects.

## References

- Alfredsen, K., C. Haas, J.A. Thuthan, and P. Zinke (2018), Brief Communication: Mapping river ice using drones and structure from motion, *The Cryosphere* **12**, 627–633, DOI: 10.5194/tc-12-627-2018.
- Alfredsen, K., A. Dalsgård, S. Shamsaliei, J.H. Halleraker, and O.E. Gundersen (2021), Towards an automatic characterization of riverscape development by deep learning, *River Res. Appl.* **38**, 4, 810–816, DOI: 10.1002/rra.3927.
- Brekke, I. (2020), Modelling av terskelfjerning og terskelendringer i Nea [Modelling weir removal in river Nea], MSc Thesis, Norwegian University of Science and Technology (in Norwegian).
- Juarez, A., A. Adeva-Bustos, K. Alfredsen, and B.O. Dønnum (2019), Performance of a two-dimensional hydraulic model for the evaluation of stranding areas and characterization of rapid fluctuations in hydropeaking rivers, *Water* **11**, 2, 201, DOI: 10.3390/w11020201.
- Junker-Köhler, B., and H. Sundt (2021), Assessing visual preferences of the local public for environmental mitigation measures of hydropower impacts—does point-of-view location make a difference? *Water* **13**, 21, 2985, DOI: 10.3390/w13212985.
- Rødtang, E., K. Alfredsen, and A. Juárez (2021), Drone surveying of volumetric ice growth in a steep river, *Front. Remote Sens.* **2**, 767073, DOI: 10.3389/frsen.2021.767073.

Received 9 May 2022  
Accepted 16 May 2022

## **A Picture Speaks a Thousand Words: Remote Sensing in Ecohydraulics**

Antóin M. O’SULLIVAN

University of New Brunswick, Fredericton, New Brunswick, Canada

Canadian Rivers Institute, Fredericton, New Brunswick, Canada

O’Sullivan Ecohydraulics Inc., Fredericton, New Brunswick, Canada

✉ aosulliv@unb.ca

### **Abstract**

The camera has a storied history, with the oldest recorded camera, the camera obscura, linked to Han Chinese philosopher Mozi *c.* 470–390 BC. Today, cameras (or sensors) are omnipresent, floating around the Earth acquiring data, gazing into space as we seek to explain our universe, and rest in your hand as you photograph a stream. In Earth science sensors are providing deep insights into hydrologic, geologic, ecologic, and hydraulic processes. In this talk I will provide an overview of the physics that underlies sensors, followed by a suite of remote sensing case studies relevant to ecohydraulic researchers, practitioners, and resource managers. These studies illustrate the utility of remote sensing for ecohydraulic studies at the catchment to patch scale, and from a snap shot in time to 10-minute resolution data collected throughout a summer.

**Keywords:** behavioural thermoregulation, hydraulic habitats, multi-scale, optical bathymetry, thermal infrared.

Received 9 May 2022

Accepted 16 May 2022



# Remote Sensing of River Temperature in a Changing Climate: from Knowledge to Applied River Management

Stephen DUGDALE

School of Geography, University of Nottingham, Nottingham, UK

✉ [stephen.dugdale@nottingham.ac.uk](mailto:stephen.dugdale@nottingham.ac.uk)

## Abstract

Climate change is increasing river temperature globally, with potentially serious consequences for iconic cold water fish species. As a result, the past 20 years have seen a considerable growth in the use of thermal and optical remote sensing (thermal infrared and otherwise) to characterise stream temperature patterns across multiple spatio-temporal scales. In this keynote, I review how remote sensing has generated new insights into our understanding of the processes driving stream temperature and explain how knowledge stemming from this research is advancing the management of rivers and streams threatened by climate change. I then examine recent advances and knowledge gaps in the field. Finally, I outline how and where progress is still needed in order to improve management of the thermal regimes of rivers, with a view to ensuring the continued survival of threatened river ecosystems.

**Keywords:** climate change, water temperature, thermal imaging, river management, fluvial ecosystems.

Received 9 May 2022  
Accepted 16 May 2022



# Can You Hear Me Now? An Overview of Telemetry Technologies and Their Applications

Nicholas J. PORTER

Merck Animal Health, Boise, Idaho, USA

✉ [nicholas.porter@merck.com](mailto:nicholas.porter@merck.com)

## Abstract

Telemetry is an ever-evolving field with a suite of technologies for wildlife and fisheries researchers. Over the past 100 years many advancements in telemetry equipment have transpired. These developments allow for numerous options when deciding on equipment and methods for telemetry related studies. As such, this talk will cover the four major divisions of telemetry including radio, acoustic, GPS, and radio frequency identification (RFID). An overview of telemetry technologies and their applications will be covered, to further education and bolster the tools that researchers and managers have at their disposal. It is the purpose of this presentation to provide guidelines and suggestions to researchers to identify when the appropriate technology should be utilized, and what combinations of these technologies are best suited for answering research questions.

**Keywords:** telemetry, remote sensing, wildlife, fish, tracking.

Received 9 May 2022

Accepted 16 May 2022



# Hydraulic Modeling of a Glacial Lake Outburst Flood (GLOF) Scenario at the River Biya

Lisa SCHMALFUSS<sup>1,✉</sup>, Martin SCHLETTERER<sup>2</sup>, and Christoph HAUER<sup>1</sup>

<sup>1</sup>Institute of Hydraulic Engineering and River Research,  
University of Natural Resources and Applied Life Sciences, Vienna, Austria

<sup>2</sup>Institute of Hydrobiology and Aquatic Ecosystem Management,  
University of Natural Resources and Applied Life Sciences, Vienna, Austria

✉ lisa.schmalfuss@boku.ac.at

## Abstract

Climate change is increasing the severity of numerous natural hazard processes: rising global air temperatures have, over the past decades, led to an acceleration of glacial retreat in many places around the world, causing increases in volume at many existing glacial lakes and the development of new ones. The increased risk of glacial lake outburst floods (GLOFs) endangers human infrastructure downstream. Hydraulic modeling is a vital tool in the process of GLOF risk assessment. The affected areas are usually difficult to access, hence the model inputs are often derived from remote sensing. The present study simulates a major scale GLOF event at the River Biya in the Siberian Altai Mountains. The propagation of possible hydrographs was modeled alongside mobilized grain sizes. Results like these can be used to anticipate the extent of a flood event of a certain magnitude and to evaluate whether any infrastructure is endangered.

**Keywords:** GLOF, cataclysmic flood, remote sensing.

## 1. INTRODUCTION

Like other parts of the Altai Mountains, part of the Biya's 300 km channel was shaped by a cataclysmic flood event triggered by the outburst of Lake Teletskoye about 37.5 thousand years ago (Baryshnikov et al. 2016). The aim of this study was to simulate flood wave propagation of this major scale scenario mobilized grainsizes as indicators for the damage potential of such

an event. The river geometry was generated from modern day ASTER GDEM (v3) and is used as a basis for hydraulic modeling (HECRAS 5.0.7) of the reconstructed GLOF scenario.

## 2. RESULTS AND DISCUSSION

The simulated GLOF hydrograph was designed as a symmetric linear rise/fall hydrograph (Watson et al. 2015) with a peak of  $2 \text{ Mio m}^3\text{s}^{-1}$  and a duration of the rising stage of 7 h to approximate the estimated total release volume of around  $49 \text{ km}^3$  of the event (main scenario, Section 2.1). Flood wave propagation was modeled for nine additional scenarios (see Section 2.2).

### 2.1 Modeling results of the ‘main scenario’ (inflow peak: $2 \text{ Mio m}^3\text{s}^{-1}$ )

Figure 1A shows the spatiotemporal development of the modeled GLOF-wave. The white dashed lines illustrate the difference between the inflow (peak:  $2 \text{ Mio m}^3\text{s}^{-1}$ ) and outflow (peak:  $1.03 \text{ m}^3\text{s}^{-1}$ ) hydrograph. There are clear retention effects, mainly between rkm 120 and 230.

The critical diameter ( $D_{50}$ ) for sediment movement of coarse materials (Fig. 1B: upper Biya) was estimated using depth and velocity information from the HEC-RAS simulations based on the approach described by Van Rijn (2019). Figure 1B gives an impression of the force of the simulated GLOF events that is particularly strong within the narrowest, steepest section in the beginning of the upper Biya, where the simulated flood wave has the potential to mobilize rocks of diameters higher than 15 m.

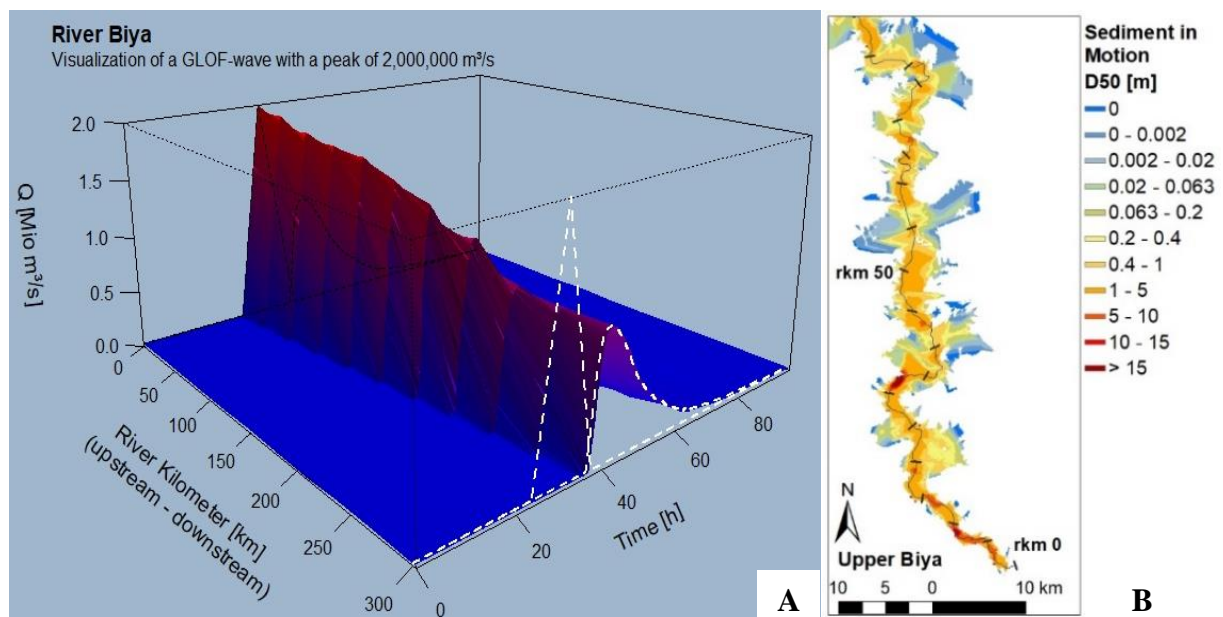


Fig. 1. Modeling results of the performed GLOF simulations.

### 2.2 Other results

In total, simulations for ten hydrographs were performed. These hydrographs differ from each other regarding peak discharge and duration. They were designed, to represent comparable scenarios regarding total release volume approximating the described GLOF scenario. While the peak of the moderate simulation scenario ( $0.3 \text{ Mio m}^3\text{s}^{-1}$ ) was only reduced by 12%, the simulated peak reduction of the most extreme scenario ( $3 \text{ Mio m}^3\text{s}^{-1}$ ) amounted to 61% (Table 1).

Table 1  
Modeled hydrograph scenarios (peak of the inflow hydrograph vs. reduction at the outflow)

Peak Q (in)	[Mio m <sup>3</sup> s <sup>-1</sup> ]	3	2.7	2.25	2	1.75	1.5	1	0.75	0.5	0.3
Peak reduction	[%]	61	58	53	48	44	41	28	26	17	12

#### References

- Baryshnikov, G., A. Panin, and G. Adamiec (2016), Geochronology of the late Pleistocene catastrophic Biya debris flow and the Lake Teletskoye formation, Altai Region, Southern Siberia, *Int. Geol. Rev.* **58**, 14, 1780–1794, DOI: 10.1080/00206814.2015.1062733.
- Van Rijn, L.C. (2019), Critical movement of large rocks in currents and waves, *Int. J. Sediment Res.* **34**, 4, 387–398, DOI: 10.1016/j.ijsrc.2018.12.005.
- Watson, C.S., J. Carrivick, and D. Quincey (2015), An improved method to represent DEM uncertainty in glacial lake outburst flood propagation using stochastic simulations, *J. Hydrol.* **529**, 3, 1373–1389, DOI: 10.1016/j.jhydrol.2015.08.046.

Received 9 May 2022  
Accepted 16 May 2022



# Integrating Remote Sensing and 2D Hydraulic Modelling for Meso-habitat Modelling in the Aurino, a Gravel-bed Alpine River

David FARÒ<sup>1,✉</sup>, Katharina BAUMGARTNER<sup>2</sup>, Robert KLAR<sup>2</sup>, Andrea ANDREOLI<sup>3</sup>,

Francesco COMITI<sup>3</sup>, Markus AUFLEGER<sup>2</sup>, and Guido ZOLEZZI<sup>1</sup>

<sup>1</sup>Department of Civil, Environmental and Mechanical Engineering, University of Trento, Trento, Italy

<sup>2</sup>Unit of Hydraulic Engineering, University of Innsbruck, Innsbruck, Austria

<sup>3</sup>Faculty of Science and Technology, Free University of Bozen-Bolzano, Bolzano, Italy

✉ david.faro@unitn.it

## Abstract

Integration of remote sensing and 2D hydraulic modelling offers the potential for broader applicability of habitat modelling at the meso-scale, extending applications to larger non-wadeable streams, and allowing to survey longer river stretches. We present an example of the application of a methodological framework for meso-scale habitat suitability modelling, on a reach of the gravel-bed Aurino River (NE Italy). The framework implements the following main steps: remote sensing-based acquisition of the topo-bathymetry and a high-resolution orthophoto; 2D hydraulic modelling coupled with an unsupervised algorithm to map hydro-morphologically defined units; semi-automated mapping of substrate and refugia; and finally, the estimation of meso-scale habitat suitabilities for a target species or community.

**Keywords:** UAV; hydro-morphological units; bathymetric LiDAR; fish habitat.

## 1. INTRODUCTION

Meso-scale habitat models have become widely accepted to quantify the impact of hydro-morphological pressures and of river restoration measures, as well as to support the definition of environmental flows. Integrating remote sensing (RS) surveys with 2D hydraulic modelling can help overcome some of the issues that limit a broader applicability of meso-scale habitat modelling: the requirement of repeated surveys at a number of streamflows, which can be very time consuming; the surveying effort, which limits the maximum size of the surveyable reach; the challenge of conducting in-stream surveys in large and non-wadeable rivers.

## 2. MODELLING FRAMEWORK

The modelling framework integrates RS and 2D hydraulic modelling to map meso-scale fish habitat suitabilities (Fig. 1). In this contribution, we present an example for a 750 m reach of a recently restored meandering section of the Aurino River (NE Italy). The workflow implements: RS-based survey of the topo-bathymetry (in the form of a DTM, acquired via Airborne LiDAR Bathymetry) and the acquisition of a high-resolution RGB orthophoto (acquired with a drone); 2D hydraulic modelling to numerically estimate the distribution of water depth and velocity at a number of discharges; the outputs of the 2D hydraulic model are used to automatically map hydro-morphologically defined units (following the procedure described in Farò et al. 2022); a semi-automated approach to describe the spatial distribution of non-hydraulic habitat descriptors (e.g. substrate and flow refugia) from the orthophoto; and finally, the estimation of meso-scale habitat suitabilities, used to derive the habitat – flow rating curves, according to the MesoHABSIM methodology (Veza et al. 2014).

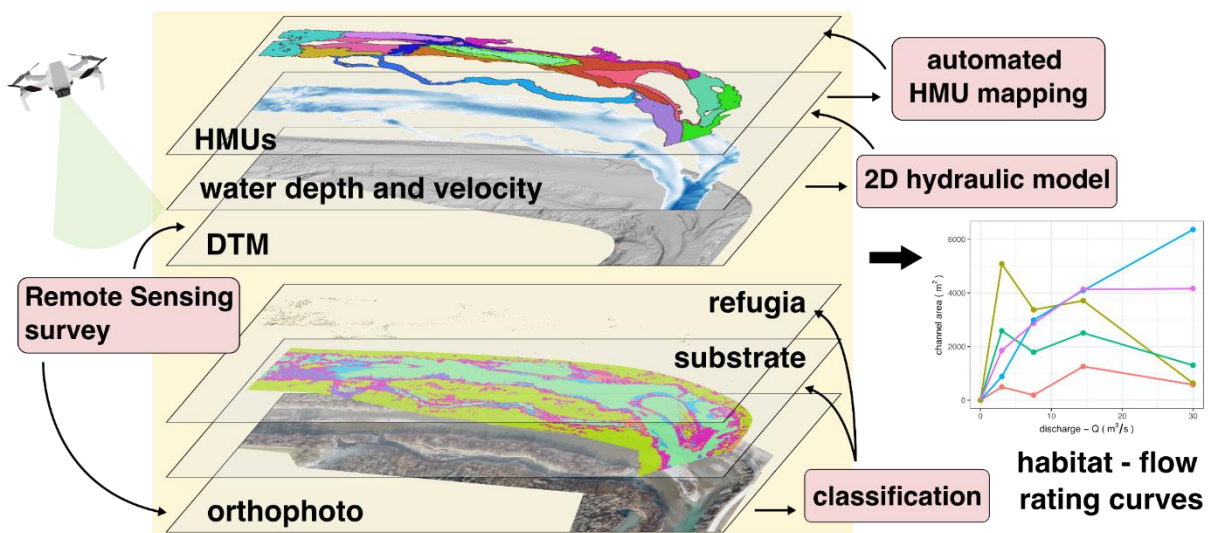


Fig. 1. Modelling framework (and examples from the Aurino reach).

## 3. CONCLUSION

We show the potential of combining RS and 2D hydraulic modelling coupled with automated procedures to map meso-scale hydro-morphologically defined units and habitat descriptors to derive fish suitability maps and hence habitat-flow rating curves. The presented framework allows objective and repeatable surveys on large gravel bed rivers, with lower surveying effort, making it possible to increase the modelled reach size, survey non-wadeable in-stream conditions, and potentially increasing the number of habitat modelling applications.

**Acknowledgments.** Financial support was received by MIUR (grant L.232/2016) and by the Autonomous Province of Bolzano/Bozen (FHARMOR project, funding agreement n. 17/34 of 03/11/2016).

## References

- Farò, D., K. Baumgartner, P. Vezza, and G. Zolezzi (2022), A novel unsupervised method for assessing mesoscale river habitat structure and suitability from 2D hydraulic models (under review).
- Vezza, P., P. Parasiewicz, M. Spairani, and C. Comoglio (2014), Habitat modeling in high-gradient streams: the mesoscale approach and application, *Ecol. Appl.* **24**, 4, 844–861, DOI: 10.1890/11-2066.1.

Received 9 May 2022  
Accepted 16 May 2022



# Deep Learning Approach for River Hydro-morphodynamics Monitoring using SAR Data

Massimiliano GARGIULO<sup>1,✉</sup>, Carmela CAVALLO<sup>2</sup>, Maria Nicolina PAPA<sup>2</sup>,  
Giuseppe RUELLO<sup>1</sup>, and Michael NONES<sup>3</sup>

<sup>1</sup>Department of Information Technology and Electrical Engineering,  
University of Napoli “Federico II”, Napoli, Italy

<sup>2</sup>Department of Civil Engineering, University of Salerno, Fisciano (SA), Italy

<sup>3</sup>Institute of Geophysics, Polish Academy of Sciences, Warsaw, Poland

✉ massimiliano.gargiulo@unina.it

## Abstract

The knowledge of the hydro-morphological evolution of lowland rivers is essential to develop integrated river management plans. Multispectral and Synthetic Aperture Radar (SAR) Satellite data can be helpful in continuous and efficient monitoring of wet channel evolutions. On the one part, multispectral images are easily interpreted but affected by the presence of cloud cover. Instead, although the SAR images have more complex interpretation, they can provide information in all weather conditions. In this work, a supervised deep learning segmentation method was proposed to analyse the hydro-morphological changes along a reach of the Italian Po River using Sentinel-1 SAR data.

**Keywords:** deep learning methods, river monitoring, Sentinel-1, Cosmo-SkyMed, wet channel evolutions.

## 1. INTRODUCTION

The continuous monitoring of fluvial dynamics is essential to know past evolutionary trends and associated drivers, to help water managers and decision-makers in managing hydro-morphology alterations of rivers. Satellite data can provide an effective and cost-effective tool to identify the optimal management practices in the river ecological status and the mitigation of hydraulic risk (Cavallo et al. 2021).

In this work, we used Sentinel-2 (S2) multispectral images with a spatial resolution of 10 m, C-band Sentinel-1 (S1) SAR images in VV and VH polarisations with 10-m spatial resolution. Specifically, the case study is a sediment bar of the Po River (Italy) near the Boschina Island (Ostiglia), characterized by frequent and relevant morphological changes.

## 2. PROPOSED DEEP LEARNING METHOD

Since Convolutional Neural Networks (CNNs) can approximate complex non-linear functions and has limited computation time thanks to the GPU usage, their usage obtained an increasing interest in many remote sensing applications (Kattenborn et al. 2021; Rezaee et al. 2018). As a drawback, the training phase requires the availability of a large amount of data. In this work, we have used a W-Net architecture that is composed by a cascade of two U-Nets, as described in Gargiulo et al. (2020). In the supervised learning, we needed to produce training examples, specifically input-target pairs. In detail, after the chain of pre-elaborations of S1 images as described in Filippini (2019), a deep learning architecture was trained starting from the S1 input data, considering as target the water masks extracted from the S2 images. The definition of proper cost functions and learning optimization algorithms is necessary in the learning phase. In this work, we used a cost function, based on Intersection-over-Union (IoU), and for the optimization algorithm the ADAM method, that is an adaptive version of the Stochastic Gradient Descent (SGD). Once the network was trained, it was tested on some of the dates in which very high-resolution images were available.

## 3. RESULTS

In Fig. 1, the qualitative comparison of the results provided by the deep learning method using Sentinel-1 data with very a high-resolution multispectral image (Fig. 1a) is reported.

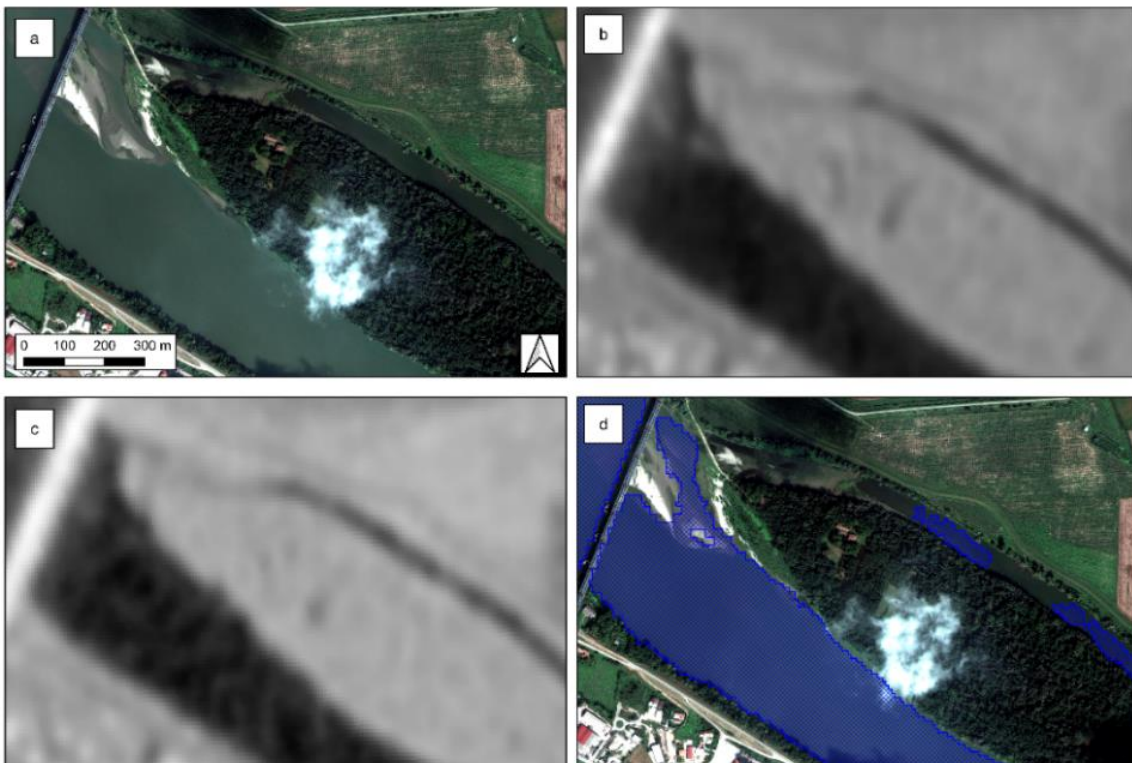


Fig. 1: (a) RGB Geo-Eye-01 (© TPMO 2020) of 16 September 2018 (H= 13.29 m a.s.l.), (b) VV polarization of Sentinel-1 images of 16 September 2018, (c) VH polarization of Sentinel-1 images of 16 September 2018, and (d) the water mask extracted by deep learning algorithm.

As observed in Fig. 1, the co-polarized images (Fig. 1b) are more informative than the cross-polarized (Fig. 1c) in separating between sediments and water pixels. However, both polarizations were useful for extracting the water masks. The water masks extracted from the deep learning algorithm tracks the wet channel with good accuracy (Fig. 1d). Similar considerations can be obtained for the different areas and different dates evaluated.

#### 4. CONCLUSIONS

In this work we have tested a deep learning approach in wet channel monitoring, and we have shown very promising results benefiting by the use of SAR data. The benefits can be more evident in future works, using the X-band Cosmo-SkyMed SAR data images in HH polarisation with 3-m as target of the deep learning method. The achieved results encourage us to exploit a segmentation solution with different features of the riverscape, e.g., sediment bars and vegetation.

#### References

- Cavallo, C., M. Nones, M.N. Papa, M. Gargiulo, and G. Ruello (2021), Monitoring the morphological evolution of a reach of the Italian Po River using multispectral satellite imagery and stage data, *Geocarto Int.*, 1–23, DOI: 10.1080/10106049.2021.2002431.
- Filipponi, F. (2019), Sentinel-1 GRD preprocessing workflow, *Proceedings* **18**, 1, 11, DOI: 10.3390/ECRS-3-06201.
- Gargiulo, M., D.A.G. Dell’Aglia, A. Iodice, D. Riccio, and G. Ruello (2020), Integration of Sentinel-1 and Sentinel-2 data for land cover mapping using W-Net, *Sensors* **20**, 10, 2969, DOI: 10.3390/s20102969.
- Kattenborn, T., J. Leitloff, F. Schiefer, and S. Hinz (2021), Review on Convolutional Neural Networks (CNN) in vegetation remote sensing, *ISPRS J. Photogramm. Remote Sens.* **173**, 24–49, DOI: 10.1016/j.isprsjprs.2020.12.010.
- Rezaee, M., M. Mahdianpari, Y. Zhang, and B. Salehi (2018), Deep convolutional neural network for complex wetland classification using optical remote sensing imagery, *IEEE J. Sel. Top. Appl. Earth Observ. Remote Sens.* **11**, 9, 3030–3039, DOI: 10.1109/JSTARS.2018.2846178.

Received 9 May 2022  
Accepted 16 May 2022



# Accurate Estimation of Water Temperature from UAV-mounted Thermal Camera: the Use of Generalized Additive Models and Dynamic Programming Algorithm to Correct for Vignetting Effect and Thermal Shift

Matteo REDANA✉ and Lesley T. LANCASTER

University of Aberdeen, School of Biological Science, Aberdeen, United Kingdom

✉ r02mr18@abdn.ac.uk

## Abstract

Water temperature maps based on Unmanned Aerial Vehicles (UAVs)-thermal camera data have a significant role to study freshwater systems and inform for the potential thermal effects of any alteration. Nevertheless, the estimation of water absolute temperature ( $T_k$ ) can still represent a problem when the accuracy needed must be  $< 1$  °C. The vignetting effect and the thermal shift are two sources of bias in the estimation of water temperature. We present here a procedure that implement already developed methodologies with new techniques to produce thermal map with errors below 1 °C.

**Keywords:** freshwater, temperature, vignetting effect, thermal shift, UAVs.

## 1. INTRODUCTION

Unmanned Aerial Vehicles (UAVs) equipped with uncooled radiometric thermal cameras are accessible tools to explore rivers' water temperature with unprecedented resolution. Nevertheless, the estimations of absolute water temperature ( $T_k$ ) can still represent a problem if is needed a high accuracy (i.e., error  $< 1$  °C). Two significative sources of bias of the recorded thermal radiation are the so-called vignetting effect (i.e., the reduction of thermal radiation intensity towards the edges of the frame) and thermal shift\drift (i.e., the variation of the overall brightness temperature of the frame due to camera heating or internal camera correction) (Abolt et al. 2018); they can determine errors in estimation of water  $T_k$  up to 8 °C (Dugdale et al. 2019). The vignetting effect can be correct through the subtraction of a correction raster obtained in field using sources of uniform temperature (i.e., camera cap or thermal blackbody), but has been

showed that the magnitude of vignetting effect can be air temperature and flight altitude dependent (Aragon et al. 2020). Thermal shift correction are based on field  $T_k$  measurement of points of known location or post processing approaches (Casas-Mulet et al. 2020; Abolt et al. 2018). The aim of our work is to implement already developed methods of correction with Generalized Additive Models (GAMs) for vignetting effect and dynamic programming for thermal shift correction in order to: (I) correct for the vignetting effect considering its dependence from flight conditions in field; (II) correct for the thermal shift (or any fictitious variation of background temperature) with a post-processing method that release any assumption of thermal shift linearity and do not request extensive deployment of loggers other than the validation ones; (III) result in a final estimation of  $T_k$  with errors  $< 1$  °C. The results here presented are based on four sets of radiometric JPG images (RJPG) captured with the DJI Zenmuse XT2 radiometric camera (640×512) over the Errochty Water and the Braan River (Scotland). Ten loggers were placed in the water for validation purposes during the flight.

## 2. VIGNETTING CORRECTION

Similarly to Abolt et al. (2018) the vignetting correction is performed by adding to each thermal image a correction raster (i.e., a raster which pixels values compensate the decreasing of thermal radiation due to vignetting) built using one of the frames captured by the drone during the flight (i.e., accounting for altitude and temperature effect). Specifically, it must be selected a frame with a relatively homogenous temperature (e.g., forest cover, water or grass field), and model its pixels raw value through a GAM with the form

$$\text{raw}_i = f(x_i, y_i), \quad (1)$$

where  $f$  is a thin plate splines with 100 knots and  $x, y$  is the position of the  $i$ th pixel. The relatively small number of knots has been chosen to capture the “overall trend” of the pixels’ raw values variation and thus the vignetting effect. The pixels’ value of the correction raster is computed as the difference between the maximum GAM-predicted pixels’ value (assumed to be the point unaffected by vignetting) and each GAM-predicted pixel value.

## 3. THERMAL SHIFT CORRECTION

Vignetting corrected images are then imported in Agisoft Metashape producing an orthomosaic. Orthophotos are subsequently exported. We developed a dynamic programming algorithm, that generates thermal shift correction starting from a single corrected orthophoto (i.e., an orthophoto which scene include one of the deployed loggers and thus corrected in its raw values based on the logger’s water  $T_k$  measurement during flight); subsequent images are iteratively corrected by compensate the difference in their mean raw value (computed on the overlapping part of the orthophotos) with already corrected images.

## 4. VALIDATION

Using vignetting and shift corrected images we built a final orthomosaic where the estimated  $T_k$  was validated using the average  $T_k$  recorded by validation loggers during flight (excluding the logger used in the shift correction). Specifically, we computed Mean Absolute Error (MAE), the Errors standard deviations (E-sd), the Root Mean Square Error (RMSE), and the correlation coefficient ( $r$ ). In all the four dataset MAE  $< 0.7$  °C, E-sd  $< 0.55$  °C, RMSE  $< 0.53$  °C, and  $r > 0.91$ .

**Acknowledgments:** We thank NERC Field Spectroscopy Facility (FSF) of Edinburgh to the loan of the radiometric and UAV equipment, including cameras, and the expertise offered to complete this study.

## References

- Abolt, C., T. Caldwell, B. Wolaver, and H. Pai (2018), Unmanned aerial vehicle-based monitoring of groundwater inputs to surface waters using an economical thermal infrared camera, *Opt. Eng.* **57**, 5, 053113, DOI: 10.1117/1.oe.57.5.053113.
- Aragon, B., K. Johansen, S. Parkes, Y. Malbeteau, S. Al-Mashharawi, T. Al-Amoudi, C.F. Andrade, D. Turner, A. Lucieer, and M.F. McCabe (2020), A calibration procedure for field and UAV-based uncooled thermal infrared instruments, *Sensors* **20**, 11, 3316, 1–24, DOI: 10.3390/s20113316.
- Casas-Mulet, R., J. Pander, D. Ryu, M.J. Stewardson, and J. Geist (2020), Unmanned Aerial Vehicle (UAV)-based Thermal Infra-Red (TIR) and optical imagery reveals multi-spatial scale controls of cold-water areas over a groundwater-dominated riverscape, *Front. Environ. Sci.* **8**, 64, 1–16, DOI: 10.3389/fenvs.2020.00064.
- Dugdale, S.J., Ch.A. Kelleher, I.A. Malcolm, S. Caldwell, and D.M. Hannah (2019), Assessing the potential of drone-based thermal infrared imagery for quantifying river temperature heterogeneity, *Hydrol. Process.* **33**, 7, 1152–63, DOI: 10.1002/hyp.13395.

Received 9 May 2022  
Accepted 16 May 2022



# Geographical Information System Based Morphometric Analysis of Dibang River, Arunachal Pradesh, India

Abhishek Bamby ALPHONSE<sup>1,✉</sup> and Kusuma KILINGAR NADUMANE<sup>2</sup>

<sup>1</sup>Institute of Geophysics, Polish Academy of Sciences, Warsaw, Poland

<sup>2</sup>Pondicherry University, Puducherry, India

✉ balphonse@igf.edu.pl

## Abstract

Geoprocessing techniques in GIS allow extraction of the river basin and its drainage networks, thus facilitating the computation of morphometric parameters of the basin. Multi Error Removed Improved Terrain (MERIT) DEM based delineation of the watershed of the Dibang River Basin and its sub-basins in the north-eastern Indian state of Arunachal Pradesh along with its drainage networks was attempted in this study using geospatial tools. Also, various morphometric parameters that describe the basin characteristics and morphotectonic parameters were derived. According to the Strahler's scheme, the Dibang River is a seventh order stream with a catchment area of 11823.9 km<sup>2</sup>. Dri, Mathun, Emra, Ithun, Ahul, and Tangon are the major tributaries of the Dibang River. Various morphometric parameters show the dominant tectonic influence in the drainage development in the area. The morphometric parameters indicative of tectonic influences correlates well with the regional tectonics when compared with the lineament map and lithotectonic map.

**Keywords:** morphometric analysis, Geographic Information System, geomorphology, Dibang River, Dibang Multipurpose Project.

## 1. INTRODUCTION

The Dibang Multipurpose Project (3000 MW) is being planned on the Dibang River (Fig. 1), which flows from the snow-capped southern flank of the Himalayas near the Tibet border at an elevation of nearly 5000 meters. The dam is about 1.5 kilometers upstream from the junction of the Ashu Pani and Dibang rivers, and 43 kilometers from Roing. Morphometric analysis is the quantitative measurement configuration of the surface of the earth in terms of shape and dimension of the landforms (Babar 2005). The morphological analysis of a river basin and its fluvial processes play a vital role in deciphering the river's geohydrological characteristics and

express its climate, geological conditions, geomorphology, and structural (faults, joints, etc.) aspects of its catchment. The factors that play in the development of the watershed will be correlated with its shape, size, relief, the slope of the catchment, number and length of drainage channels, drainage density, etc. (Rastogi and Sharma 1976). It allows quantifying the geometry of the river basin which in turn provides insight into the underlying lithology, differences in rock hardness and its erodibility, structural controls, recent regional or local diastrophism (Strahler 1964). The morphometric analysis of the river provides an insight of the hydrological behavior of the river when the dam is constructed.

The basin morphometric parameters are broadly classified into linear, areal, relief, and aspects. Parameters under linear aspects describe the relationship between stream order, number, and length whereas the aerial aspects are computed to describe the shape and also understand the relationship of the stream length and number over the catchment development. Relief aspects give an idea about the erosive power of the streams and the amount of the mass to be eroded to reach the base level profile, the slope of the hills that determine the surface runoff. Quantitative morphometric analysis has been in wide use for prioritizing sub-watersheds for better management planning and practices in different parts of the world (Sangma and Guru 2020). The interplay of tectonics and drainage basin morphologies is widely used as an identification tool in tectonic geomorphology (Bull and McFadden 1977; Burbank and Anderson 2001).

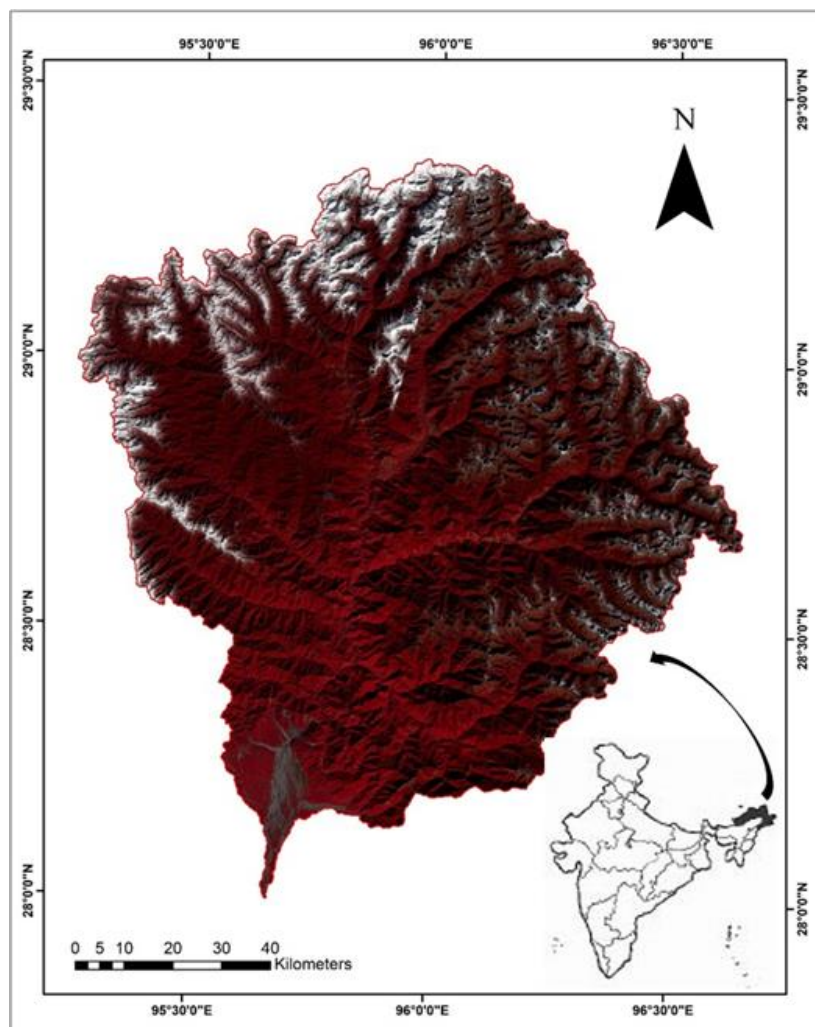


Fig. 1. Location of the Dibang River Basin.

## 2. DATA AND METHODOLOGY

The data used in the study include Landsat 8 Operational Land Imager (OLI) satellite imagery, Multi Error Removed Improved Terrain DEM (MERIT DEM), published lithotectonic maps, and the earthquake epicenter data adopted from United States Geological Survey, USGS (<http://earthquake.usgs.gov/earthquakes/search/>). Landsat8 OLI data is multispectral satellite imagery with 9 spectral bands: Band 1 to Band 9. OLI bands 1 to 7 represent coastal, blue, green, red, NIR, SWIR-1, and SWIR-2 bands with a spatial resolution of 30 m. Band 8 represents a Panchromatic band with a spatial resolution of 15 m. Band 9 represents a cirrus band with a spatial resolution of 30 m. Further details about the OLI imagery can be obtained from the website: <https://landsat.gsfc.nasa.gov/landsat-8/landsat-8-overview>. MERIT DEM (Yamazaki et al. 2017) represents the terrain elevations at a 3-arc second resolution. It was developed by removing multiple error components (absolute bias, strip noise, speckle noise, and tree height bias) from existing spaceborne DEM's (SRTM3 v2.1 and AW3D-30m v1). MERIT DEM was downloaded from [http://hydro.iis.u-tokyo.ac.jp/~yamadai/MERIT\\_DEM/](http://hydro.iis.u-tokyo.ac.jp/~yamadai/MERIT_DEM/).

The study involves carrying out morphometric analysis of the Dibang River Basin to understand the hydrological and morphotectonic signature of the basin. The morphometric analysis of the Dibang River Basin was carried out using the MERIT DEM. Arcmap 10.2 software has been used to analyze the morphometric parameters. The software's hydrology toolset has been used to extract the basin and the corresponding drainage network and to derive the morphometric parameters. The various morphometric parameters derived to understand the linear (Stream Order, Stream Number, Stream Length, Stream Length Ratio, Mean Bifurcation Ratio), Aerial (Stream Length Index, Basin Length, Basin Area, Drainage Density, Stream Frequency, Elongation Ratio, Circulatory Ratio, Form Factor, Drainage Texture), Relief (Relief, Relief Ratio, Slope), and Morphotectonic (Hypsometric Integral, Sinuosity, Asymmetry Factor, Valley Width to Height Ratio) aspects of the basin. Further, the longitudinal profiles of the river channels were derived using Global Mapper 21.1 software. The results of morphotectonic parameters were correlated with the lineament map interpreted from the Landsat8 OLI False color image and the shaded relief map of the region using visual interpretation techniques and on-screen digitization. The published lithotectonic map of the area was also used for making the inferences. The study highlights the strong influence of tectonics in the development of drainage basin, which can be inferred from the morphotectonic parameters and longitudinal profile.

## References

- Babar, M. (2005). *Hydrogeomorphology: Fundamental, Applications and Techniques*, New India Publishing Agency, New Delhi, 288 pp.
- Bull, W.B., and L.D. McFadden (1977), Tectonic geomorphology north and south of the Garlock Fault, California. **In:** D.O. Doehring (ed.), *Geomorphology in Arid Regions: Binghamton Geomorphology Symposium 8*, Routledge, London, 115–138.
- Burbank, D.W., and R.S. Anderson (2001), Geomorphic markers. **In:** D.W. Burbank and R.S. Anderson, *Tectonic Geomorphology*, Blackwell Publishing, 13–32.
- Rastogi, R.A., and T.C. Sharma (1976), Quantitative analysis of drainage basin characteristics, *J. Soil Water Conserv. India* **26**, 1–4, 18–25.
- Sangma, F., and B. Guru (2020), Watersheds characteristics and prioritization using morphometric parameters and Fuzzy Analytical Hierarchical Process (FAHP): A part of Lower Subansiri Sub-Basin, *J. Indian Soc. Remote Sens.* **48**, 473–496, DOI: 10.1007/s12524-019-01091-6.

- Strahler, A.N. (1964), Quantitative geomorphology of drainage basins and channel networks. **In:** V.T. Chow (ed.), *Handbook of Applied Hydrology*, McGraw-Hill, New York, 4.39–4.76.
- Yamazaki, D., D. Ikeshima, R. Tawatari, T. Yamaguchi, F. O’Loughlin, J.C. Neal, C.C. Sampson, S. Kanae, and P.D. Bates (2017), A high-accuracy map of global terrain elevations, *Geophys. Res. Lett.* **44**, 11, 5844–5853, DOI: 10.1002/2017GL072874.

Received 9 May 2022  
Accepted 16 May 2022

## Mapping Riparian Vegetation and Hydromorphology with UAS and Machine Learning

Björn BASCHEK<sup>1,✉</sup>, Edvinas ROMMEL<sup>1</sup>, Frederik KATHÖFER<sup>1</sup>, Laura GIESE<sup>1</sup>,  
Katharina FRICKE<sup>1</sup>, Tina MÖLTER<sup>2</sup>, Filip DZUNIC<sup>2</sup>, Maryam ASGARI<sup>3</sup>, Paul NÄTHE<sup>4</sup>,  
Paul DEFFERT<sup>2</sup>, Rock GILLES<sup>2</sup>, Jens BONGARTZ<sup>3</sup>, Andreas BURKART<sup>4</sup>,  
Maïke HEUNER<sup>1</sup>, Ina QUICK<sup>1</sup>, and Uwe SCHRÖDER<sup>1</sup>

<sup>1</sup>Federal Institute of Hydrology, Koblenz, Germany

<sup>2</sup>Geicoptix, Trier, Germany

<sup>3</sup>University of Applied Sciences, Koblenz, Germany

<sup>4</sup>JB Hyperspectral Devices, Düsseldorf, Germany

✉ mdrones4rivers@bafg.de

### Abstract

Sustainable management of riparian zones requires detailed spatial information about vegetation and hydromorphological properties. Uncrewed aerial systems (UAS) or gyrocopters equipped with multispectral cameras yield imagery of small to intermediate scale areas. Machine learning classification workflows (object based, random forest) including additional geodata and trained with in-situ data allow to map classes of vegetation and hydromorphological substrate types with different level of detail. A case study was carried out in a floodplain area along the River Rhine, Germany, resulting in overall accuracies for UAS data of 89% for basic surface types, 88% for vegetation units, 75% for dominant stand, and 62% for substrate types. Classification probability maps helped to identify areas of lower classification performance, as e.g. vegetation within the transition zone, thus allowing for a subsequent, more focused and effective site inspection. In combination, this workflow provides a valuable tool for monitoring and ecologically integrated water management.

**Keywords:** floodplain vegetation, river, remote sensing, OBIA, classification.

## 1. INTRODUCTION

River floodplains are hotspots of biodiversity and at the same time affected by human activities, especially along regulated waterways used for transportation. Flooding and water availability drive the small-scale distribution of vegetation communities.

A sustainable management of waterways requires sufficient data on vegetation and hydro-morphological substrate types and structures. Though numerous person-days are spent on field surveys, spatial data is often insufficient, in particular in inaccessible areas. Imagery acquired by uncrewed aerial systems (UAS) in combination with suitable processing algorithms can be an efficient tool to gain information about ecosystems and to reduce time spent on in-situ data acquisition to a minimum.

The joined research project “mDRONES4rivers” had the aim to fine-tune data acquisition methods for river floodplains in Germany. Using as an example the nature reserve Emmericher Ward, Rhine River, Germany, this case study proposes a classification framework for UAS or gyrocopter imagery focusing on vegetation units and outlines a combined mapping approach with UAS or gyrocopter and field data.

More detailed background information on related literature, methodology and results can be found in Rommel et. al. (2022).

## 2. METHODOLOGY

Multiple indices and texture measurements were calculated based on 5 cm resolution, multi-spectral UAS imagery (red, green, blue, red-edge, near infrared; MicaSense RedEdge-M on a DJI Phantom 4 Pro UAS). Alongside this data a flood duration model and a digital surface model were used to apply an object-based image analysis (OBIA) workflow. Processing steps included segmentation, feature selection, hyperparameter tuning, model fitting, and evaluation.

Following segmentation, basic surface types were classified, distinguishing between vegetated areas, substrate types and water (6 classes, 1st level). Based hereon, vegetation was further classified in units found in riparian zones (5 classes, 2nd level) and dominant stands (19 classes, 3rd level). In parallel, substrate types were divided into 7 classes, 2nd level. The classification was implemented using Random Forest (RF) algorithm with tuned hyperparameters for each level.

Training and validation of the classification models was performed based on in-situ data, which was collected parallel to flight survey and afterwards expanded by using processed orthophotos. Following a bootstrap approach 500 models were built with different combinations of training and validation data. Probability maps were produced by class membership probabilities automatically estimated within the RF classification.

## 3. RESULTS

High overall accuracies (OA) were achieved for basic surface types (OA = 89%) and vegetation units (OA = 88%). Dominant stand and substrate type classification resulted in OA of 75% and 62%. The results for dominant stands are species dependent. Especially in the case of strongly fragmented stands and not surprisingly for small training samples classification accuracies are low. However, for well-developed stands mostly formed by big species satisfactory results are achieved.

The proposed approach for future monitoring activities is to reduce the need of additional in-situ and in image training data by including existing data from similar riparian zone areas. For larger areas (up to 40 km<sup>2</sup>/h), gyrocopter can be used – though in that case more in-situ data for (pre-)training is required as producing additional training data from orthophotos is more difficult due to typically reduced resolution. By including auxiliary data and acquiring UAS or gyrocopter data, classification and probability maps are to be produced. By combining them as

well as adding knowledge about achievable accuracies for individual target classes of classification and making them available in field on a handheld device, a concluding on-site investigation can be planned in an efficient way by putting focus, e.g. on areas of low performance probability but high user relevance.

Thus, our results provide a valuable step using robust machine learning algorithms to develop an efficient monitoring tool for applied water management.

**Acknowledgments.** The authors are thankful to the German Federal Ministry for Digital and Transport and the mFUND for funding the project mDRONES4rivers (FKZ: 19F2054).

#### References

Rommel, E., L. Giese, K. Fricke, F. Kathöfer, M. Heuner, T. Mölter, P. Deffert, M. Asgari, P. Nätke, F. Dzunic, G. Rock, J. Bongartz, A. Burkart, I. Quick, U. Schröder, and B. Baschek (2022), Very high-resolution imagery and machine learning for detailed mapping of riparian vegetation and substrate types, *Remote Sens.* **14**, 4, 954, DOI: 10.3390/rs14040954.

Data availability: <https://zenodo.org/search?q=mDRONES4rivers>

Received 9 May 2022  
Accepted 16 May 2022



# Modelling Vegetation Condition using a Water Balance Model and Long Short-Term Memory Networks on a Floodplain Receiving Environmental Water

Chunying WU<sup>1,2,3,✉</sup>, Michael J. STEWARDSON<sup>1</sup>, J. Angus WEBB<sup>1</sup>, and Stefan NORRA<sup>3</sup>

<sup>1</sup>Department of Infrastructure Engineering, Faculty of Engineering and IT,  
The University of Melbourne, Melbourne, Australia

<sup>2</sup>Australian-German Climate & Energy College, The University of Melbourne, Melbourne, Australia

<sup>3</sup>Institute of Applied Geosciences, Karlsruhe Institute of Technology, Karlsruhe, Germany

✉ chunyingw@student.unimelb.edu.au

## Abstract

Environmental water is delivered to floodplains to maintain environmental health in terms of vegetation health and animal populations in arid and semi-arid areas. When and how much environmental water is required to restore or maintain vegetation health requires robust predictions of vegetation response. We used Normalized Differences Vegetation Index (NDVI) derived from 30-year Landsat dataset to represent vegetation condition. A lake water balance model and long short-term memory networks (LSTMs) were coupled to model NDVI. The predictor variables included in the LSTMs are the outputs of the water balance model, climate factors, day of year and previous NDVI values. The model is expected to generate more precise predictions of ecological outcomes under different watering scenarios, and thus has the potential to help environmental water management in the changing climate.

**Keywords:** environmental water, long short-term memory networks (LSTMs), Normalized Differences Vegetation Index (NDVI), floodplain, Hattah lakes.

## 1. INTRODUCTION

River floodplains are at risk of degradation because of human activities, river regulation and climate change. To restore and protect floodplain ecosystems, environmental water delivery programs have been implemented around the world. These programs are implemented through engineering-based approaches including inundating floodplains by pumping into canals and

then controlling water delivery with regulators to mimic flood events (Wu et al. 2022). The long-term temporal and spatial impact of environmental water for floodplain vegetation has been studied in several semi-arid floodplains in Australia (Wu et al. 2022; Merritt et al. 2010; Thapa et al. 2019). However, previous research has only been done using simple empirical models that do not take hydrological dynamics of floodplain watering sufficiently into account. Using hydrological models would allow us to consider the environmental water volume, flow path and release timing when predicting vegetation condition.

The objective of this study is to construct a model to predict NDVI taking environmental water volume and climate factors into consideration, using Hattah Lakes, north-western Victoria, Australia as a case study. In this research, a lake water balance model is being constructed that considers precipitation, environmental water, lake volume change and evaporation, using a 16-day time step over 30 years. The output of the water balance model combined with precipitation, temperature, evapotranspiration, day of year and previous NDVI, will be used as predictor variables of Long Short-Term Memory networks (LSTMs). LSTMs are deep learning models that have a long-term memory, making them suitable for time series predictions (Reddy and Prasad 2018). The model can be used to verify the effectiveness of environmental water strategies and support environmental water management under the changing climate.

## 2. LAKE WATER BALANCE MODEL AND LSTMS

### 2.1 Lake water balance model

Inputs to the water balance model of the floodplain lakes include precipitation, natural floods, and environmental water; the outputs include the change in lake volume and evaporation. The difference between outputs and inputs is considering as a change in soil and groundwater. Because the environmental water is transferred to lakes through a creek and are not able to inundate the vegetation area, it is therefore influencing vegetation through lateral flow of soil water.

The following equations show the lake water balance model under two conditions, environmental water being delivered, or natural floods occurring. In these equations,  $\Delta gw$  represents change in soil and groundwater,  $P$  represents precipitation,  $Ew$  is environmental water volume staying into the system,  $Nf$  is natural floods volume into the system, and  $\Delta Vl$  stands for volume change in Hattah Lakes. The environmental water volume can be extracted from records of the input regulators and output regulators. For the natural floods volume, it is considered as a function of discharge in the River Murray at the Euston regulator upstream of Hattah Lakes and the maximum capacity of Chalka creek – the channel through which environmental water is delivered – (1.04 m<sup>3</sup>/s) will be used.

$$\Delta gw = P + Ew - Ev - \Delta Vl \quad \text{when environmental water occurs} \quad (1)$$

$$\Delta gw = P + Nf - Ev - \Delta Vl \quad \text{when natural floods occurs} \quad (2)$$

### 2.2 LSTMs

LSTM is an artificial recurrent neural network architecture with a long-term memory. In recent years, LSTMs has been successfully applied to many studies involving time series prediction (Li et al. 2017). They have also been used to make NDVI predictions and displayed superior performance to other traditional neural networks (Reddy and Prasad 2018). Therefore, LSTMs are being used in this study to improve NDVI prediction using hydrological and climate factors. Due to the 16-day resolution of Landsat, there are 571 samples, 399 of them will be used as training data, 114 samples will be used as validation data and others will be used for testing. Pixel gaps because of cloud were interpolated from the previous and following images.

### 2.3 Expected results

The constructed model will provide robust NDVI predictions for different environmental water or natural floods situation under changing climate. Therefore, environmental water can be managed more precisely and effectively to support vegetation growth in floodplain.

#### References

- Li, X., L. Peng, X. Yao, S. Cui, Y. Hu, C. You, and T. Chi (2017), Long short-term memory neural network for air pollutant concentration predictions: Method development and evaluation, *Environ. Pollut.* **231**, 1, 997–1004, DOI: 10.1016/j.envpol.2017.08.114.
- Merritt, D.M., M.L. Scott, N. LeRoy Poff, G.T. Auble, and D.A. Lytle (2010), Theory, methods and tools for determining environmental flows for riparian vegetation: riparian vegetation-flow response guilds, *Freshwater Biol.* **55**, 1, 206–225, DOI: 10.1111/j.1365-2427.2009.02206.x.
- Reddy, D.S., and P.R.C. Prasad (2018), Prediction of vegetation dynamics using NDVI time series data and LSTM, *Model. Earth Syst. Environ.* **4**, 409–419, DOI: 10.1007/s40808-018-0431-3.
- Thapa, R., M.C. Thoms, M. Reid, and M. Parsons (2019), Do adaptive cycles of floodplain vegetation response to inundation differ among vegetation communities? *River Res. Appl.* **36**, 4, 553–566, DOI: 10.1002/rra.3538.
- Wu, C., J.A. Webb, and M.J. Stewardson (2022), Modelling impacts of environmental water on vegetation of a semi-arid floodplain–lakes system using 30-year Landsat data, *Remote Sens.* **14**, 3, 708, DOI: 10.3390/rs14030708.

Received 9 May 2022  
Accepted 16 May 2022



# Evaluation of Restoration Projects with Hyperspatial Remote Sensing of Fish Habitat using an Unmanned Aerial Vehicle (UAV)

Lukas KIRCHGÄSSNER<sup>1,✉</sup> and Günther UNFER<sup>2</sup>

<sup>1</sup>blatffisch e.U. – Consultants in Aquatic Ecology and Engineering, Wels, Austria

<sup>2</sup>Institute of Hydrobiology and Ecosystem Management,  
University of Natural Resources and Life Sciences, Vienna, Austria

✉ kirchgaessner@blatffisch.at

## Abstract

We developed a method to provide a relatively simple, quick and inexpensive assessment of restoration success in relation to fish fauna. Using a UAV, high-resolution orthomosaics of three restored and three channelized river sections were created under low, medium, and high flow situations. These served as the basis for remote mapping of fish habitats, focusing on riffle and shallow water areas as potential spawning and juvenile and hence key habitats for rheophilic fish species. It was found that by interpreting high-resolution orthomosaics, it was possible to map these habitats, whose actual suitability was validated with field observations. Together with an analysis of discharge time series (17 years), the mapped habitat situations were related to the probability of their occurrence. By combining morphological and hydrological analyses of the restoration projects, it was possible to assess whether the newly created habitats were usable all year round or only at certain flow situations.

**Keywords:** UAV, fish habitat mapping, restoration, hydropeaking.

## 1. INTRODUCTION

The evaluation of river restoration projects is very important (Bash and Ryan 2002) to enhance the effectiveness of future attempts. Regarding the fish fauna, there is common agreement that a rehabilitation of key habitats of the target community is necessary for long-term improvement. For rheophilic fish species in Europe, both spawning and juvenile habitats are considered key habitats (Person et al. 2014). It is thus reasonable to assume that restoration actions that restore

these key habitats are more likely to have a positive effect on the fish community than those that do not.

Traditionally, river habitat assessment is carried out in the field. However, it is more and more supplemented by methods of aerial image interpretation and other remote sensing techniques. Especially Unmanned Aerial Vehicles (UAVs) provide an easy, cost-effective alternative to traditional habitat mapping (Carbonneau and Piégay 2012).

In this work, a UAV was used to map fish habitats at three restored and three channelized river sections in Austria. One study site is located at the river Ybbs in Lower Austria, which shows a nivo-pluvial flow regime. The other two sites are located at the river Enns in Styria (moderate nival flow regime), one of which is heavily affected by hydropeaking. In addition, discharge time series were analyzed to relate the mapped habitat situations to the probability of occurrence of the documented flow situations.

## 2. DESCRIPTION OF THE METHOD

### 2.1 Habitat mapping

Aerial imagery was acquired with the UAV model DJI Phantom 4 RTK at an altitude of 60 m. The generated orthomosaics had a spatial resolution of 1.9 cm. For each restoration site, a channelized river section of equal length was chosen as comparison site. At each site, surveys were conducted at multiple flow situations, ranging from low to high flow. The mapping was done in the GIS-software QGIS. Fish habitat was digitized manually on mesohabitat-level by visual interpretation. The mapped mesohabitats consisted of riffles, shallow areas, pools and runs. Riffles and shallows were assigned the fish-ecological function as potential spawning and larval/juvenile habitats for rheophilic fish species. As ground-truth data, coloured metal discs were placed on the river bottom before the UAV survey. At each disc, water depth was measured, which later helped in the visual estimation of different water depths. Additionally, the mapped potential juvenile habitats were validated with traditional visual mapping of juvenile fish in these areas. We hereby were able to outline habitat availability both quali- and quantitatively.

### 2.2 Discharge analysis

To investigate the probability of the documented situations, discharge time series (2002–2018, 15 min) were obtained from the gauging stations closest to study sites. These were split into three discharge periods, respectively, according to the life cycle of the European grayling (*Thymallus thymallus*), whereas “spawning and incubation” included all data from March–May, “early juvenile” all data from May–July, and “late juvenile” all data from August–October. For these periods, flow-duration curves were calculated. These enabled to estimate the share of time the documented flow situations were exceeded, which was set as exceedance probability.

## 3. RESULTS AND CONCLUSION

The restoration at the Ybbs is considered a complete success, as the recreated spawning and juvenile habitats are available in high proportions at all flow situations, even at higher discharges with a rather low probability of occurrence.

The first studied restoration at the Enns led to an increase in spawning habitat. Juvenile habitat however remains a bottleneck as it is massively decreased at higher flows, which, however, are typical in the early phase of the life cycle of grayling due to the nival flow regime.

At the second studied restoration at the Enns, potential spawning and juvenile habitats have been recreated. However, because of sub-daily flow fluctuations due to hydropeaking, they are instable and hence not permanently available for fish. For example, 79% of newly created shallow water areas are dewatered in about 20% of the time and are therefore impose a high risk of stranding juvenile fish. These findings are summarized in Fig. 1.

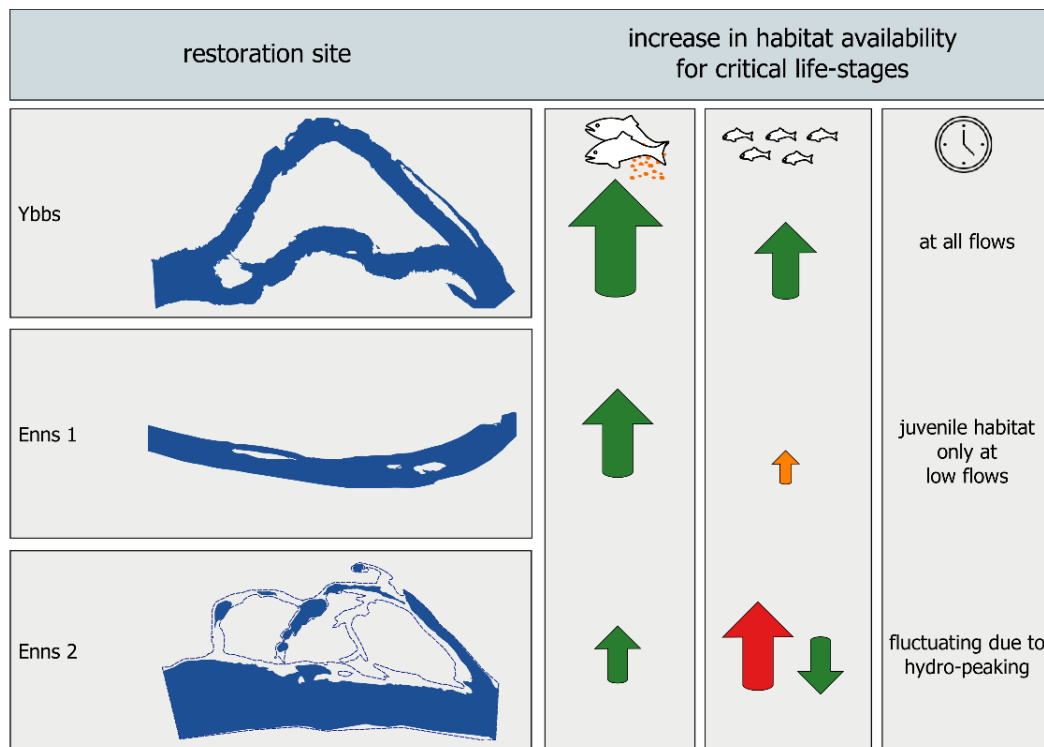


Fig. 1. Increase in habitat availability for critical life-stages of rheophilic species at the investigated restoration sites. Color code of arrows: green – permanently available habitat, orange – only at certain flows, red – temporarily available with stranding risk. The size of the arrows indicates the increase in habitat availability compared to a channelized reference site, following a space-for-time substitution.

With the chosen combination of morphological and hydrological assessments we were able to get a better understanding of fish habitat availability and how it changes with changing flow conditions, e.g. due to hydro-peaking. If fish habitat is mapped only at low flow, as it is frequently done in Austria, the results might not reflect a situation which is limiting for the fish fauna. With a UAV, quantitative habitat mapping can easily be done at multiple flow situations.

#### References

- Bash, J.S., and C.M. Ryan (2002), Stream restoration and enhancement projects: is anyone monitoring?, *Environ. Manage.* **29**, 6, 877–885, DOI: 10.1007/s00267-001-0066-3.
- Carbonneau, P.E. and H. Piégay (2012), *Fluvial Remote Sensing for Science and Management*, John Wiley & Sons, Chichester.
- Person, E., M. Bieri, A. Peter, and A.J. Schleiss (2014), Mitigation measures for fish habitat improvement in Alpine rivers affected by hydropower operations, *Ecohydrology* **7**, 2, 580–599, DOI: 10.1002/eco.1380.

Received 9 May 2022  
Accepted 16 May 2022



# Experimental Study on Swimming Behaviour of Fish in an Open Channel Based on Video Recognition

Yi ZHOU, Yue ZHANG, Yu HAN<sup>✉</sup>, and Huhu LIU

China Agricultural University, State College of Water Resources & Civil Engineering, Beijing, China

✉ yhan@cau.edu.cn

## Abstract

Various forms of obstacle structures in water are common in the natural environment. The flow through these obstructions causes mutual interference, and changes in hydraulic conditions result in changes in fish swimming behaviour around the column. In this study, the behaviour of carp is evaluated when interacting with wake currents caused by three types of columns: shuttled, D-shaped, and rectangular. The hydraulic properties of the natural fish passage are simulated and analysed in coupling with the swimming behaviour of the fish. Based on two-dimensional threshold segmentation (OTSU) and video recognition, the probability of fish occurrence in different locations and the tail swing frequency can be identified. The probability of fish occurrence can be predicted by BP model when the parameters of hydrodynamic characteristics under unknown flow are known. The results show it is reliable in all three types of channels and provides a reference for finding swimming paths of fish.

**Keywords:** fish behaviour, video recognition, flow characteristics, tail swing frequency, open channel.

## 1. INTRODUCTION

Various types of barriers in the natural environment act as obstacles to fish migration routes and they pose a threat to global biodiversity (Silva et al. 2018). Lindberg et al. (2016) constructed a model to predict the path selection of Atlantic salmon and pointed out that more research should focus on the connection between turbulence intensity gradients and fish path selection (Marques et al. 2018; Terayama et al. 2017) analyzed some characteristic points or curvature of the fish to confirm the frequency of tail swing. UAV or remote sensing technology has been increasingly developed, this study is mainly based on image recognition with some deep learning models to link hydrodynamic properties with fish behaviour.

## 2. MATERIALS AND METHODS

The experimental study was conducted in an open channel. Acoustic Doppler velocimetry (ADV) was used to measure the hydraulic conditions caused by the obstacle columns. CFD numerical simulations are used to model the hydraulic properties of the rough riverbed (Fig. 1). The experimental results and numerical simulation results were verified to be correct with each other. This study uses the results of numerical simulations of the hydraulic properties. The position of the fixed camera in the experiment records the places of the fish. The experimental data of fish swimming behaviour is transformed into images, and image recognition and tracking is performed by constructing the convolutional neural network, combined with the deep learning algorithm YOLOv5 (Fig. 2). Carp are subject to fatigue and behavioural memory during the experiments, and with this, in mind, the experiments were conducted on alternate days.

The physical model test and fish swimming observation test were completed in the hydrodynamics laboratory of China Agricultural University. The open channel is a rectangular inclined tank 6.3 m long, 0.8 m wide, and 0.6 m deep. The experimental conditions were varied by adjusting the flow rate for testing. Shuttle, D-shaped and rectangular barriers are placed in the channel.

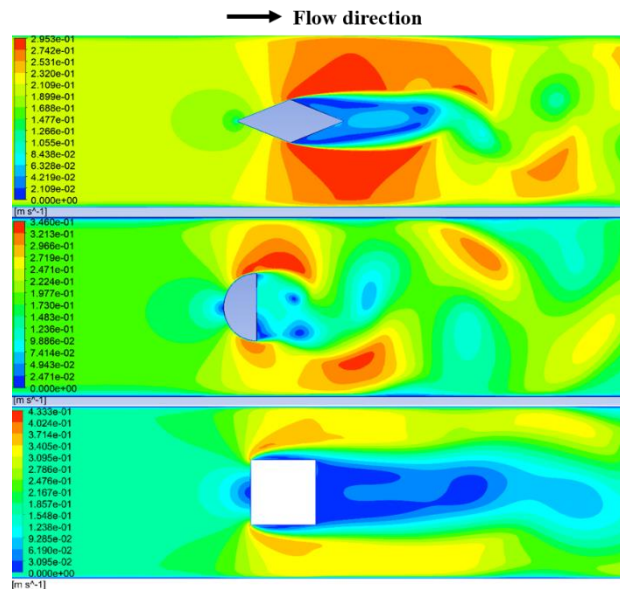


Fig. 1. Numerical simulation results for flow.

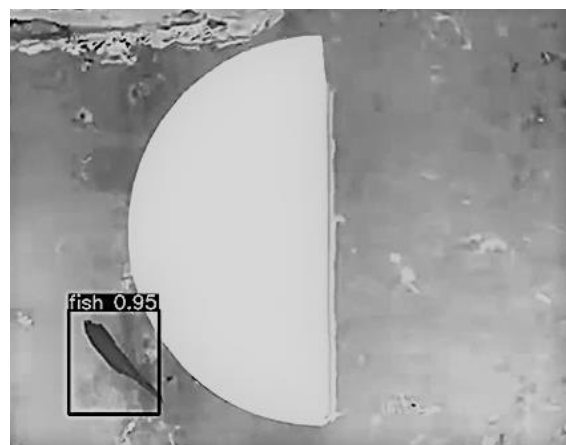


Fig. 2. Fish tracking based on video recognition.

### 3. RESULTS

Firstly the measured data verifies the correctness of the results of the numerical simulations (Fig. 3). In the subsequent analysis we therefore mainly consider the results of the simulated numerical simulations.

Based on the results of image recognition for fish, the probability of fish appearing at different locations in the channel is obtained. The results show that lower flow velocities and relatively low turbulence exist in the area behind the channel sidewalls and obstacle posts. The probability of fish occurrence was high in the area with low flow velocity and relatively low turbulence. This indicates the importance of the turbulence structure generated by the current and the water column in influencing the area and extent of fish aggregation.

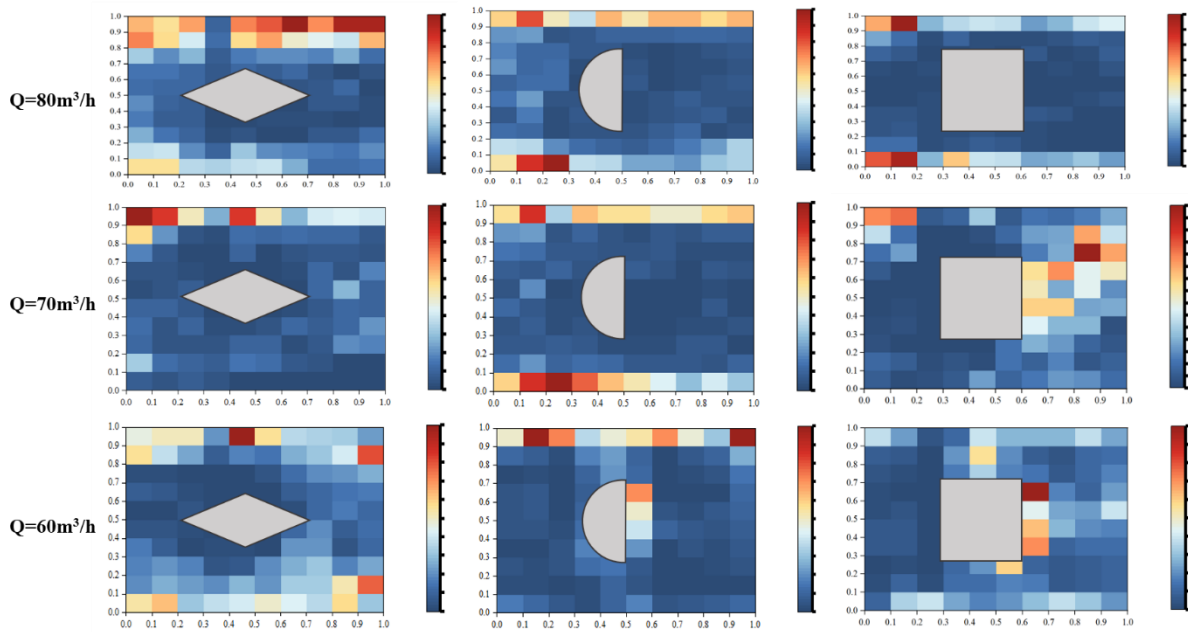


Fig. 3. Probability of fish occurrence in channels with different structural columns.

### 4. DISCUSSION

The BP neural network is a global convergence and local search optimization algorithm with strong fault tolerance and generalization ability. With flow rate  $Q$ , horizontal coordinate  $x$ , vertical coordinate  $y$ , flow velocity  $v$ , and turbulent kinetic energy TKE as input covariates. The channel is divided into 100 uniformly sized grids, and the probability of fish occurring in the grid  $P$  is the output covariate, forming a machine-learning mapping relationship. A stratified sampling approach is adopted, with 80% of the dataset used for training the machine learning model and the remaining 20%, half for testing and a half for inspection. Before training the BP neural network, the raw data is normalized to a number between 0 and 1. Figure 4 shows that the slope of the line fitted once to the measured and predicted values is close to 1. Some of the neurons are damaged by data perturbation will not have a great impact on the global training results, and the trained network can still process new or noisy contaminated data correctly.

Manual counting of the number of tail swings of carp. The 600 carp images with good quality were labeled. A two-dimensional threshold segmentation is taken to extract the foreground target fish body, and then the foreground graphics are refined to eliminate the bifurcation caused by the imperfection of the refinement algorithm to obtain a bifurcation-free fish body midline, extract the feature points on the head and tail of the fish body and the spine curve, and finally

calculate the curvature to obtain the number of tail wagging of the carp. The binary image refinement algorithm is chosen to extract the midline of the carp fish body. The mean value plus triple standard deviation of 0.003 and the empirical value of 0.005 were processed using the systematic error statistics. The following Table 1 shows the comparison between the number of tail swings calculated by the algorithm and the number of tail swings counted manually.

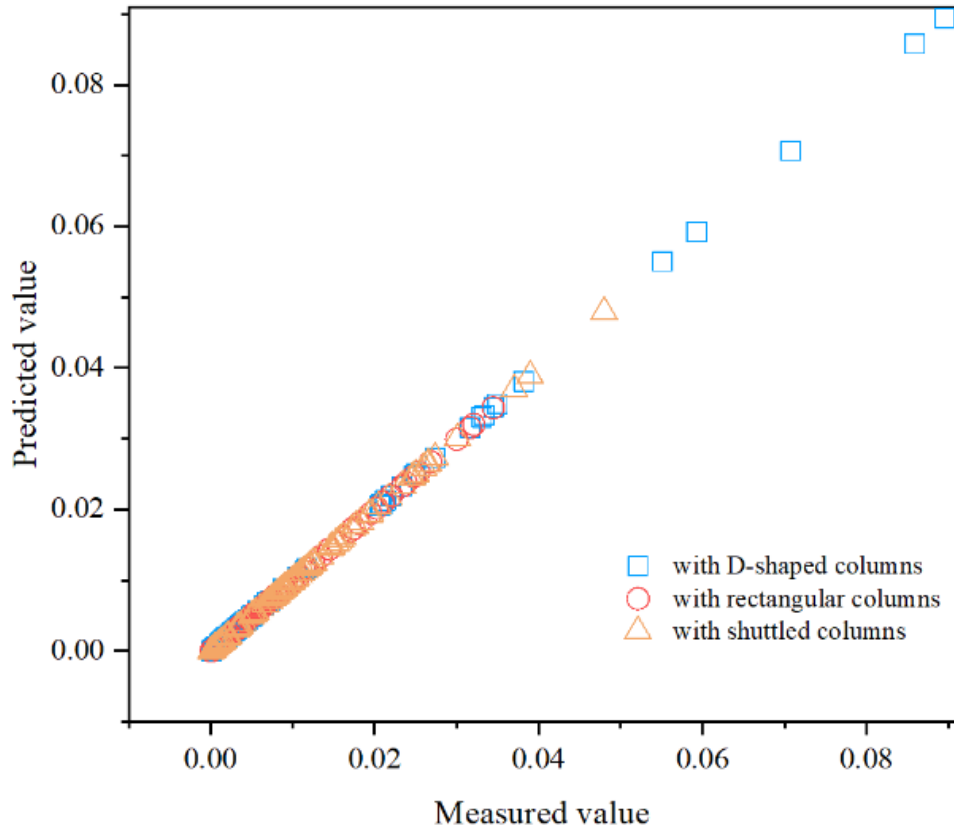


Fig. 4. Prediction results for different working conditions using BP models.

Table 1  
Fish tail swing frequency recognition results

Curvature parameter	Number of algorithm counts	Number of manual counts	Absolute error	Correct rate
0.005	95	109	15	92.9
0.005	135	144	23	91.2
0.005	167	195	31	91.9
0.005	234	253	39	92.8
0.003	55	109	10	60.0
0.003	185	144	47	62.1
0.003	102	195	11	0.58
0.003	413	253	47	0.55

## 5. CONCLUSIONS

- 1) In currents with large hydraulic structures, carp prefer to be found in locations where the flow and turbulence of the water are relatively low, and will also favor staying behind the posts.
- 2) Image recognition of fish based on YOLOv5 has high confidence, it provides a new idea for observing fish in the field. The algorithm based on two-dimensional threshold segmentation (OTSU) can identify the frequency of fish tail swing.
- 3) The BP neural network has a good overall predictive performance for the probability of fish occurrence. The use of BP models for probability prediction can be considered in practical engineering, which is useful for understanding the behaviour of fish under different flow conditions.

## References

- Lindberg, D.E., K. Leonardsson, and H. Lundqvist (2016), Path selection of Atlantic salmon (*Salmo salar*) migrating through a fishway, *River Res. Appl.* **32**, 4, 795–803, DOI: 10.1002/rra.2909.
- Marques, J.C., S. Lackner, R. Felix, and M.B. Orger (2018), Structure of the zebrafish locomotor repertoire revealed with unsupervised behavioral clustering, *Curr. Biol.* **28**, 2, 181–195.e5, DOI: 10.1016/j.cub.2017.12.002.
- Silva, A.T., M.C. Lucas, T. Castro-Santos, C. Katopodis, L.J. Baumgartner, J.D. Thiem, K. Aarestrup, P.S. Pompeu, G.C. O'Brien, D.C. Braun, N.J. Burnett, D.Z. Zhu, H.-P. Fjeldstad, T. Forseth, N. Rajaratnam, J.G. Williams, and S.J. Cooke (2018), The future of fish passage science, engineering, and practice, *Fish Fish.* **19**, 2, 340–362, DOI: 10.1111/faf.12258.
- Terayama, K., H. Hioki, and M.-a. Sakagami (2017), Measuring tail beat frequency and coast phase in school of fish for collective motion analysis. **In:** *Proc. SPIE 10225, Eighth Int. Conf. on Graphic and Image Processing (ICGIP 2016)*, DOI: 10.1117/12.2266447.

Received 9 May 2022  
Accepted 16 May 2022



# Study on Fish Swimming Behavior Based on Image Velocimetry

Huhu LIU✉, Yu HAN, Yi ZHOU, and Yue ZHANG

China Agricultural University, Haidian District, Beijing, China

✉ sy20213091843@cau.edu.cn

## Abstract

The fish passage is an effective way for fish to pass through dams and obstacles, but most fish passes are currently not used, and the energy used by fish to pass through them is too great to meet the conditions for passage. This paper focuses on the factors that affect the fish swimming energy expenditure. The factors include the hydraulic conditions of the fish passage, the fish swimming speed, and the fish tail swing frequency. A baffle is set up in a U-shaped channel with different barriers on either side of the baffle, making the hydrodynamic conditions different on each side of the channel. HD cameras were set up to observe and record the fish swimming behaviors in the channel, and deep learning YOLOV5 algorithm was used to identify the fish swimming speed and the frequency of the tail swing. The data was analyzed to derive an equation for calculating the fish swimming energy consumption. FLUENT was used to simulate the fish energy consumption in the channel during high flows and to obtain the route with the lowest energy consumption of the fish, which will provide suggestions for the subsequent construction of fish passage and fish crossing facilities.

**Keywords:** deep learning, fish swimming energy consumption equation, tail swing frequency, model simulation.

## 1. INTRODUCTION

The fish passage is an artificial channel for fish to travel upstream through a structure such as a lock or dam or a natural structure. The ecological significance of the fish passage is to mitigate the impact of dam construction on fish and to help impeded fish to pass through the barrier and reach their important habitat for breeding and overwintering. At present fish passages are not working very well (Cao et al. 2016). The fish use too much energy to swim in them to meet the conditions for their passage and therefore the fish passages are not working as well as they could.

Fish accomplish most of their basic behaviors by swimming. The fish swimming behaviors can be influenced by hydrodynamic conditions in the channel. Additionally, the active metabolic rate (AMR) is a valuable parameter that can be used as an indicator of the fish swimming efficiency (Xia et al. 2013). Ohlberger et al. (2006) analyzed the relationship between the fish

swimming speed and AMR in the channel and derive the equation (Ohlberger et al. 2005, 2006). This paper focuses on the relationship between the fish energy consumption and the hydraulic conditions in the channel and the fish own factors, and get the fish swimming energy consumption equation.

## 2. EXPERIMENTAL SET UP

A baffle in the U-shaped channel divides the channel into two identical parts, with different barriers on each side, making the hydrodynamic conditions different on each side (Kerr et al. 2016). Instantaneous flow velocities and water depths are measured at multiple cross sections. Turbulent kinetic energy is obtained using these data. A HD camera was set up at the upper end of the observation area to observe and record the fish swimming behaviors in the channel.

### 2.1 Animals

The fish used in the experiment is *Cyprinus Carpio haematopterus*, a freshwater fish belonging to the cyprinid family, which is an active omnivorous fish and easy to observe. Thus it is widely used in biological research. And a pre-experiment was needed to determine the state of adaptation of the fish in the channel and to take valid data for analysis.

### 2.2 Deep learning

The camera takes the image sequence of fish swimming, and YOLOV5 uses the image processing technology to analyze the image. Then the computer establishes the mapping relationship between the pixel coordinates of the image and the coordinates of corresponding points in space through calibration. It can obtain the fish actual displacement in a short time, so as to calculate the fish swimming speed.

A fish tail swing action is taken as the initial movement and the recognition number is taken as the number of swimming tail swing. So the fish tail swing frequency is obtained by combining the number of fish tail swing and the fish swimming time.

## 3. DIMENSIONAL ANALYSIS

The fish swimming energy expenditure is related to the fish swimming speed (Ohlberger et al. 2005, 2006), tail swing frequency (Chen et al. 2009), fish length (Marras et al. 2015), flow velocity, water depth, turbulent kinetic energy, etc. The fish swimming energy expenditure can be expressed by the following functional equation.

$$F(J, U, H, TKE, f, m, v, l) = 0 ,$$

where  $J$  is the joule,  $f$  is the tail swing frequency,  $U$  is the flow velocity,  $H$  is the water depth, TKE is the turbulent kinetic energy,  $m$  is the fish weight,  $v$  is the fish swimming speed, and  $l$  is the fish length. Based on the  $\pi$  theorem, using  $l$ ,  $v$ ,  $m$ , as the fundamental physical quantities, the above equation can be expressed in dimensionless form as follows:

$$F = \left( \frac{J}{mv^2}, \frac{U}{v}, \frac{H}{l}, \frac{TKE}{v^2}, \frac{fl}{v} \right)$$

Ohlberger et al. (2006) analyzed the relationship between the fish swimming speed and AMR in the channel. The fish weight is 100 g and fish length is 10 cm, so the AMR equation is:

$$AMR = U^{2.53} \times 2.33 + 10 .$$

Consider the AMR as the fish swimming energy consumed expenditure.

$$\frac{J}{mv^2} = \left(\frac{U}{v}\right)^x \left(\frac{H}{l}\right)^y \left(\frac{TKE}{v^2}\right)^z \left(\frac{f\Delta}{v}\right)^w$$

All parameters can be obtained through instrumentation and calculation. Use these parameters to get  $x$ ,  $y$ ,  $z$ ,  $w$  and the fish swimming energy consumption equation is derived.

#### 4. DISCUSSION

The fish swimming energy consumption in the channel when high flow occurs in the channel is simulated by FLUENT. The route that consumes the least amount of energy for the fish is get. Fish swimming energy consumption equation can be used to inform the construction of fish passage and fish crossing facilities.

#### References

- Cao, N., Z.G. Zhong, X.H. Cao, S.L. Zhang, and Y.C. Zhang (2016), Status of fishway construction in China and typical case analysis, *Water Resour. Protect.* **32**, 6, 156–162.
- Chen, J.J., G. Xiao, X.F. Ying, and H.B. Zhou (2009), Fish activity model based on tail swing frequency, *J. Image Graph.* **14**, 10, 2177–2180.
- Kerr, J.R., C. Manes, and P.S. Kemp (2016), Assessing hydrodynamic space use of brown trout, *Salmo trutta*, in a complex flow environment: a return to first principles, *J. Exp. Biol.* **219**, 21, 3480–3491, DOI: 10.1242/jeb.134775.
- Marras, S., S.S. Killen, J. Lindström, D.J. McKenzie, J.F. Steffensen, and P. Domenici (2015), Fish swimming in schools save energy regardless of their spatial position, *Behav. Ecol. Sociobiol.* **69**, 2, 219–226, DOI: 10.1007/s00265-014-1834-4.
- Ohlberger, J., G. Staaks, P.L.M. Van Dijk, and F. Holker (2005), Modelling energetic costs of fish swimming, *J. Exp. Zool. A* **303A**, 8, 657–664, DOI: 10.1002/jez.a.181.
- Ohlberger, J., G. Staaks, and F. Holker (2006), Swimming efficiency and the influence of morphology on swimming costs in fishes, *J. Comp. Physiol. B* **176**, 1, 17–25, DOI: 10.1007/s00360-005-0024-0.
- Xia, J.G., S.J. Fu, Z.D. Cao, J.L. Peng, J. Peng, T.T. Dai, and L.L. Cheng (2013), Ecotoxicological effects of waterborne PFOS exposure on swimming performance and energy expenditure in juvenile goldfish (*Carassius auratus*), *J. Environ. Sci.* **25**, 8, 1672–1679, DOI: 10.1016/S1001-0742(12)60219-8.

Received 9 May 2022  
Accepted 16 May 2022



# Processing of Hyperspectral Aerial Images to Characterise the Bathymetry of Rivers

Julien GODFROY<sup>1,✉</sup>, Jérôme LEJOT<sup>2</sup>, Luca DEMARCHI<sup>3</sup>, Kristell MICHEL<sup>1</sup>,  
and Hervé PIEGAY<sup>1</sup>

<sup>1</sup>Univ Lyon, ENS de Lyon, CNRS, UMR 5600 EVS, Lyon, France

<sup>2</sup>Univ Lyon, Université Lumière Lyon 2, CNRS, UMR 5600 EVS, Lyon, France

<sup>3</sup>Institute of Geodesy and Geoinformatics, Wrocław University of Environmental and Life Sciences,  
Wrocław, Poland

✉ julien.godfroy@ens-lyon.fr

## Abstract

Fluvial remote sensing of river bathymetry is crucial for characterizing the topography of the riverbed and monitor changes in habitat at large scales. Hyperspectral data enables bathymetric retrieval through optical models. On the Ain River (France), multiple hyperspectral aerial campaigns with different sensors were conducted and processed to create bathymetric maps of the river for different flow conditions. In particular, a continuous bathymetric map was produced for a 20 km reach of the river with a median error of 20 cm for depths up to 2.5 m. Despite the uncertainties of the models tested, the result are more robust spatially and over a wider range of depth and flow conditions than optical models based on traditional colour imagery.

**Keywords:** bathymetry, hyperspectral, remote sensing.

## 1. INTRODUCTION

River bathymetry is important for mapping riverbed topography at the mesohabitat scale, and to monitor channel morphology changes after restoration actions. One promising tool for bathymetric remote-sensing in river environments is hyperspectral imaging which aims at establishing an empirical optical model based on the Beer-Lambert law by linking water depth with at-sensor radiance as measured through a high number of narrow spectral wavelengths. Compared to optical bathymetric models calibrated with more traditional colour or multispectral imagery,

hyperspectral images have been shown to predict depths in deeper waters (up to 6 m), and are thought to allow for more robust depth detection (Legleiter and Fosness 2019). However, the ability of models to accurately predict bathymetry over long spatial extents (more than 10 km, and requiring several images) at different flow conditions and with different channel bottom substrates is poorly understood.

## 2. MATERIALS AND METHODS

Hyperspectral remote sensing data was acquired over the Ain River (France) during three campaigns that each used a different sensor, two in 2015 and one in 2021. One of those campaigns acquired information for a reach of 20 km while the other two focused on smaller reaches of the river (100–300 m). This data was coupled with a 2D bathymetric model built at the scale of the studied reach in order to adjust for differing discharge conditions between campaigns (low flow conditions at  $27 \text{ m}^3/\text{s}$  and mean flow conditions at  $127 \text{ m}^3/\text{s}$ ), and to provide spatially-continuous calibration and validation data for the full extent of the imaged reaches.

The dimensionality of the hyperspectral data was increased by calculating band ratios and the  $\ln()$  transform of spectral bands and their ratios. By iterating through every such wavelength combination, the strength of the linear relationship between depth and reflectance was assessed for the full spectral resolution of each sensor – discharge combination. Bathymetric maps were then produced and compared to each other and to the validation dataset in order to investigate the spatial distribution of errors along the reach.

In the case of the data available for the 20 km reach, the model was built by focusing on smaller river reaches to be able to assess the portability of site-based models to long river corridors.

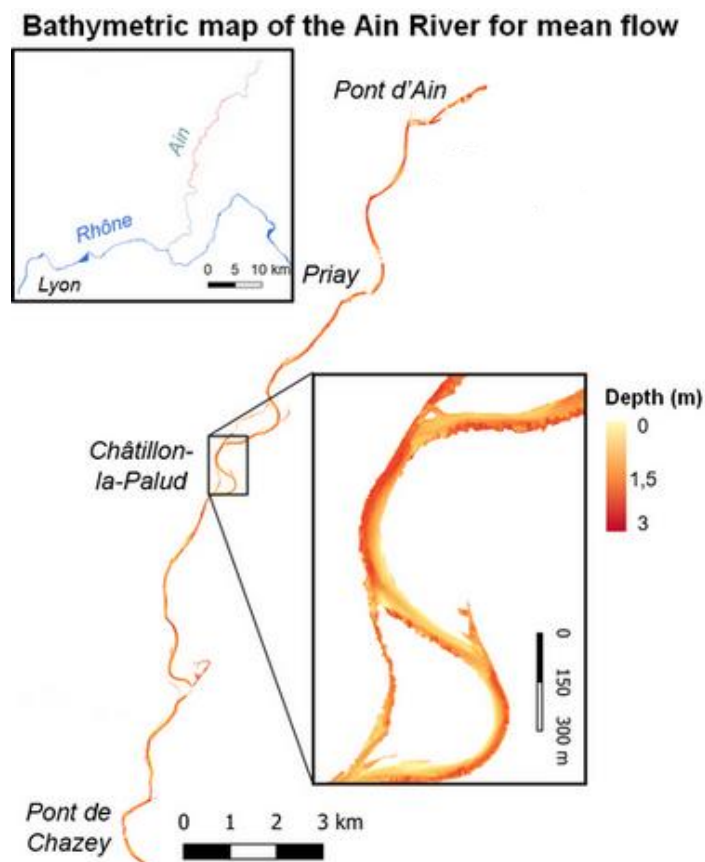


Fig. 1. Bathymetric map of the Ain River for mean annual flow conditions ( $127 \text{ m}^3/\text{s}$ ).

### 3. RESULTS

Multiple bathymetric maps were able to be built at the site-level with a high vertical accuracy ( $\sim 15$  cm). In addition, the campaign acquired under mean flow conditions ( $127 \text{ m}^3/\text{s}$ ) in 2015 was also able to predict low flow bathymetry ( $27 \text{ m}^3/\text{s}$ ) with a similar accuracy to the low flow campaign from 2015 ( $27 \text{ m}^3/\text{s}$ ).

When expanding the bathymetric models from the shorter reach to the full extent of the 20 km campaign (Fig. 1), accuracy was reduced ( $\sim 20$  cm). This reduction in accuracy is related to: (i) the presence of pool areas (5% of the study reach, depths  $> 2.5$  m at mean flow) for which quality calibration – validation information was not available, (ii) the presence of glint and turbulence on the water surface, and (iii) vegetation shadows. In addition, (iv) changes in the water column and the riverbed properties led to errors for some wavelengths combinations, but not others. Therefore, the best bathymetric model for a given reach may not always be the one with the strongest correlation to the calibration data because the range of good bathymetric models may be narrower in practice.

**Acknowledgments.** We express our gratitude to the European Facility for Airborne Research for funding one of the hyperspectral data acquisition. We also thank the NERC Airborne Research and Survey Facility for the use of some of their equipment and sensors. This research was carried out as part of a PhD funded by the School of Integrated Watershed Sciences in Lyon, and the Agence de l'Eau Rhône Méditerranée Corse.

#### References

Legleiter, C.J., and R.L. Fosness (2019), Defining the limits of spectrally based bathymetric mapping on a large river, *Remote Sens.* **11**, 6, 665, DOI : 10.3390/rs11060665.

Received 9 May 2022  
Accepted 16 May 2022

"Publications of the Institute of Geophysics, Polish Academy of Sciences: Geophysical Data Bases, Processing and Instrumentation" appears in the following series:

A – Physics of the Earth's Interior

B – Seismology

C – Geomagnetism

D – Physics of the Atmosphere

E – Hydrology (formerly Water Resources)

P – Polar Research

M – Miscellanea

Every volume has two numbers: the first one is the consecutive number of the journal and the second one (in brackets) is the current number in the series.

